

Customised fabrication of nitrogen-doped biochar for environmental applications

Zhonghao Wan¹, Yuqing Sun¹, Daniel C.W. Tsang^{1,*}, Eakalak Khan², Alex C.K. Yip³, Yun Hau Ng⁴, Jorg Rinklebe⁵, Yong Sik Ok⁶

¹ Department of Civil and Environmental Engineering, The Hong Kong Polytechnic University, Hung Hom, Kowloon, Hong Kong, China.

² Department of Civil and Environmental Engineering and Construction, University of Nevada, Las Vegas, NV 89154, USA.

³ Energy and Environmental Catalysis Group, Department of Chemical and Process Engineering, University of Canterbury, Christchurch, New Zealand.

⁴ School of Energy and Environment, City University of Hong Kong, Kowloon, Hong Kong SAR, China.

⁵ University of Wuppertal, School of Architecture and Civil Engineering, Laboratory of Soil- and Groundwater-Management, Pauluskirchstraße 7, 42285, Wuppertal, Germany.

⁶ Korea Biochar Research Centre, O-Jeong Eco-Resilience Institute (OJERI) & Division of Environmental Science and Ecological Engineering, Korea University, Seoul 02841, Republic of Korea.

*Corresponding author email: dan.tsang@polyu.edu.hk

Abstract

Global warming, environmental pollution, and energy shortage are causing severe environmental concerns worldwide. Conversion of various renewable biowastes into value-added carbon-based material can be a promising option to alleviate these issues and ensure sustainable development. The emergence of nitrogen (N)-doped biochar provides a versatile electroactive platform suitable for environmental applications. In this review, we summarise and highlight the customised productions of N-doped biochars and their applications in environmental remediation, energy storage, and biorefinery, *etc.* With a comprehensive overview of original precursor, interspecies conversion, and ultimate deactivation of various N-dopants in biochar-based carbocatalysis; their formation mechanism, distinct electrochemical characteristics, fate in the environmental applications, and electrochemical behaviours can be comprehensively analysed. Contemporary challenges that require to be addressed, and perspectives on improving N-doping technique on biochar are provided throughout the review. Overall, this review can help to cultivate new insights in the customised production of N-doped biochar for its broader applications in sustainable carbocatalysis and green chemistry.

Keywords: Engineered biochar; Nitrogen doping; Electroactive components; Advanced oxidation processes; Green catalyst; Sustainable waste management.

1. Introduction

With the overwhelming progress of industrialization and modernization, ongoing anthropogenic activities are continuously proceeding to cater for enormous demands of growing human population for various aspects including energy supply, sustenance production, municipal administration, and so forth (Cha et al., 2016; Xiong et al., 2017). Accordingly, undesired biomass wastes will be inevitably generated as by-products or residues in these energy-intensive processes (Anastopoulos et al., 2019; Demirbaş, 2000; Li et al., 2016). Vast anthropogenic and refractory biowastes, *e.g.*, agricultural waste, forestry waste, animal manure, and municipal sewage sludge (Cho et al., 2019; Xu et al., 2019a), pose a potential threat to environmental ecosystems (*e.g.*, aquatic lives, atmospheric conditions, and soil contamination), as the annual generation of biomass has notably exceeded the natural degradation capacity. These waste streams carry opportunity and financial costs and contribute to toxic leachate from landfills. In the past decades, methods involving direct incineration, anaerobic composting, aerobic fermentation, and fodder production are extensively explored; however, these methods will either produce harmful greenhouse gases or require long operational time and spatial facilities, reluctantly constructing a healthy sustainable carbon recycle (Lee et al., 2017a).

To overcome the shortcomings above, several specific processing methods such as pyrolysis (Tripathi et al., 2016), gasification (Igalavithana et al., 2019; Yang et al., 2019a; You et al., 2017), and hydrothermal treatment (Gao et al., 2018; Wang and Wang, 2019) have drawn much attention due to their win-win merits. Particularly, pyrolysis under different operational parameters (*e.g.*, retention time, peak temperature, and ramping rate) can be applied to transform lignocellulosic biomass into desired biofuels (*i.e.*, syngas and tars) (Cho et al., 2017; Yang et al., 2019b). Meanwhile, the residual black carbon, namely biochar, can be simultaneously produced as a

permanent carbon sink to reach carbon sequestration, thus to mitigate the global warming induced by carbon dioxide (CO₂) compared with the uncontrollable discharge from conventional disposal (Palansooriya et al., 2019; You et al., 2017). It has been estimated that 0.1–0.3 billion tons of CO₂ can be deducted from the natural carbon cycle *via* biochar storage (Fowles, 2007). Furthermore, the obtained biochar usually possesses well-developed porous structure and maneuverable surface chemistry, which endow the potential to act as excellent adsorbent or catalyst in a wide array of environmental applications (Bamdad et al., 2017; Kumar et al., 2020; Lee et al., 2017b). It has been widely applied in environmental decontamination (Wan et al., 2019a; Wan et al., 2019b), energy storage (Li et al., 2017), and soil amendment (Ahmad et al., 2014; Beckers et al., 2019; El-Naggar et al., 2019), *etc.* Traditional carbonaceous materials produced from coal (*e.g.*, activated carbon (AC)), and the so-called “emerging” materials, such as carbon nanotubes (CNTs) (Chen et al., 2018a), graphene oxides (GO) (Sun et al., 2012), and nanodiamond (Lee et al., 2016), *etc.*) are fascinating at the research level. Yet, their applications in industrial remain a challenge due to their complicated synthesis under harsh conditions with low yield. In contrast, a more sensible and technologically viable approach is the creative utilization of biochar produced from renewable and natural bioresource at a large scale (Wang and Wang, 2019). The emergence of biochar introduces a prospect alternative to facilitate green chemistry and sustainable applications based on vast biomass.

Although raw biochar could be directly adopted as a versatile carbon substrate, the specific surface area (SSA) and surface chemistry (*i.e.*, defective level and sp^2 -hybridized carbon framework) are limited due to the nonstoichiometric nature of original biomass (Duan et al., 2018). Proper modification processes are usually required to tailor its properties for broader use. Acid/alkaline treatment is commonly exploited as it could significantly promote SSA and surface

functionalization, providing more exposed active sites for further reactions (Cazetta et al., 2011; Rajapaksha et al., 2016). Metal incorporation could significantly combine the advantages of different transition metals (*i.e.*, ultrahigh reactivity, dense electron population, redox recycle, and magnetism) and biochar framework (*i.e.*, porous structure, catalyst dispersion, and leaching mitigation) (Cho et al., 2019; Yang et al., 2018; Yang et al., 2019c; Yi et al., 2020). Oxidizing or reductive agents were deployed on biochar to tune the surface oxygen functionalities and SSA (Wang et al., 2015a). Several activation techniques by changing purging gas from conventional inert environment (*i.e.*, Ar or N₂) to reactive substrate (*i.e.*, steam or CO₂) were also introduced to modify biochar structure (*i.e.*, micro- and mesopore evolution) (Igalavithana et al., 2019; Yang et al., 2019d). Although these techniques have been extensively explored and showed great promise in practical application; some irrevocable shortcomings hinder their footpath in green and sustainable chemistry.

The controllable introduction of desired oxygen functionalities on biochar is still a tricky challenge. Some types (*e.g.*, carboxylic group) can even exert negative influences to affect the reducibility of biochar and cause an electron-deficient nature. In contrast, metal accommodation prevails to circumvent this problem using oxygen functionalities as anchoring sites to stabilize metal centers. Nevertheless, the introduced metal centers were generally reported to suffer from unsolvable leaching and passivation, which might lead to secondary contamination irrespective of their high efficiencies (Oh and Lim, 2019). Besides, the reversible regeneration of metal centers is associated with high-temperature annealing with another stage of energy input. This inconvenient regeneration process will increase the operational cost and thus impede practical application. To sum up, a metal-free modification with low environmental concern is of considerable significance to develop the sustainable nature of biochar.

The concept of metal-free heteroatom doping has been prevalent in carbonaceous communities for several years (Ortiz-Medina et al., 2019). Doping technologies with earth-rich elements such as nitrogen (N), boron (B), and sulphur (S), were exhaustively employed for synthesizing nanocarbons. In general, it is well-acknowledged that the introduction of alien non-carbon atoms into the ordered sp^2 -hybridized carbon framework can alter the electrochemical capacities of the original π -electron networks, creating an imbalanced electroactive state in the carbon structure to deliver greater electrocatalysis (Frank et al., 2009; Yang et al., 2019e). The reactive sites can promise stronger interactions with exterior molecules to achieve various purposes. It has been reported that heteroatom doping technology, especially nitrogen doping (N-doping) with the strongest efficacy, was applied to facilitate catalysis of nanocarbons, enhance detection limit of sensors, and improve nanomaterial dispersion, *etc.*

From a chemical point of view, biochar produced under low-temperature treatment ($< 700\text{ }^{\circ}\text{C}$) with a low graphitization degree is regarded as unsuitable for doping technology (Duan et al., 2018). The graphitized biochar with a well-ordered and highly graphitized domain allowed the heteroatom doping technologies to enter the field of biochar (Zhu et al., 2018). In recent years, using biochar as fundamental carbon substrate to conduct N-doping to obtain high-performance material has been tentatively explored. Most of the relevant studies on N-doped biochar clarified that it remains a great challenge to explicitly elucidate the doping mechanism (Ding et al., 2020; Ho et al., 2019). The physicochemical properties of biochar cannot be readily tuned due to the inherent structural complexity of biochar and need further insights to construct a comprehensive system. Besides, the origin of the catalytic mechanism is still vague and poorly stated as a result of the disciplinary disparities. To unveil the underlying regularities might require exhaustive and all-round understanding into the advances of carbon communities.

Several critical reviews with focal points on metal-free carbonaceous materials for environmental applications have been put forward (Duan et al., 2018; Li et al., 2018; Liu and Dai, 2016; Miller et al., 2017). The concurrent stabilization of N and C utilizing suitable biowastes shows fascinating preponderance over non-renewable nanocarbons to practically mitigate environmental deterioration. However, these investigations neither addressed the environmental sustainability of N-doped biochar nor interconnected the scalable synthetic protocols with doping technologies to integrate disciplinary knowledge extended from mechanistic chemistry to practical engineering. Systematic and comprehensive review to summarise the integral progress of N-doped biochar in relevant practical applications is yet to be conducted. Thus, it is indispensable to put forward this critical review to guide future research in fabrications, to provide disciplinary insights on catalytic mechanisms, and to reach the wider application of this high-efficient N-doped biochar ultimately.

Herein, this review will cover the following topics: (a) fundamental characteristics of N-doping biochar and its typical N-dopants; (b) insights into the N-doping mechanism with an exhaustive investigation on the fabrication procedures of N-doped biochar; and (c) applications of N-doped biochar as adsorbent, electrocatalyst, and electrode material in different environmental fields. This review will illustrate an integral fate of N-dopants on biochar in a sequential manner from the original precursor, interspecies conversion, to ultimate attenuation/consumption. Furthermore, we address different essential and technical challenges in each section from experimental and mechanistic aspects, aiming to cultivate the customised and up-scaling production of N-doped biochar in future environmental research.

2. Formation and characteristics of different N species on biochar

In principle, the incorporated nitrogenous contents mainly involve five types: (1) aminated functionalities, (2) pyridinic N in six-membered heteroring, (3) pyrrolic N in five-membered heteroring, (4) graphitic N (namely quaternary N or sp^2 -hybridized nitrogen atom adjacent to three sp^2 -hybridized carbon atoms), and (5) oxynitrides ($-NO_x$) (Ortiz-Medina et al., 2019). The N-dopants are likely to originate from the thermal cracking of initially attached aminated functionalities. After the dehydration, condensation, and aromatization, the N atoms could be successfully incorporated into carbon units at the expense of large fraction of volatile nitrogenous contents.

Amongst, aminated functionalities (*i.e.*, primary, secondary, or tertiary amino) are functional groups attached to the carbon surface under different protonated states. Typically, the alien N content (*e.g.*, ammonia gas) will interact with the topological deviations of pristine graphitic carbon network to grow along with the anchoring defective sites *via* covalent bonding interaction. The generation of amino groups usually corresponds to the initial step to introduce N contents into a carbon framework (Mian et al., 2019; Mian et al., 2018). With an electron-rich feature from unpaired electrons, aminated groups can act as efficient adsorptive sites to enrich reactant molecules for better reactant-substrate contact. The aminated functionalities, however, are more susceptible to the oxidizing environment (Wang and Wang, 2019) and, thus, give limited catalysis compared with the doped N atoms (*i.e.*, pyridinic N, pyrrolic N, and graphitic N). Furthermore, the depletion of electrons in the aminated groups can readily generate oxynitride ($-NO_x$), which is chemically inert for many catalytic reactions (Duan et al., 2015a).

Apart from the surface aminated contents on biochar, N-dopant is more desired in redox catalysis as it is prone to disrupt the electronic and spin features of biochar framework to improve overall electrochemical capability rather than to donate electrons in a localized region. Pyridinic N and

pyrrolic N donate one and two p -electrons to the adjacent sp^2 -hybridized carbon conjugated framework to form p -type doping (Oh and Lim, 2019). Furthermore, edge-functionalized pyridinic N and pyrrolic N with unpaired electrons are considered to donate electrons to participate in redox reactions directly. The graphitic N inserted into an intact benzene ring is assigned to the sp^2 -hybridized N atom adjacent to three neighboring sp^2 -hybridized carbon atoms. The n -type graphitic N is generally regarded as the most conducive and electroactive N-dopant (Oh and Lim, 2019), which tends to interact with reactants to reduce their energy threshold to cleave/dissociate respective chemical bonds. Compared with amino and oxynitride that maintain the fundamental features of functional groups, the doped N atoms are energetically preferable to substitute the carbon atoms at the edges of an ordered carbon unit to form heteroring at atomic scale (Gao et al., 2019; Yang et al., 2019e).

With a higher electronegativity vs. adjacent carbon atom (Pauling scale: $\chi_n = 3.04 > \chi_c = 2.55$), the incorporation of these doped N atoms can induce a dipole moment, where the negatively charged N atom as basic sites fulfill redox recycle and the positively charged adjacent carbon atoms as the adsorptive sites intimately interact with exterior substances (Duan et al., 2015b; Sun et al., 2014). The electron flow would follow a decoupled stage to restore the electrochemical state of those N-dopants without irreversibly compromising the heteroatoms (Wan et al., 2020a). Besides, the electron-deficient state of carbon atoms adjacent to doped N atoms is believed to facilitate the overall reluctance of catalyst towards oxidative erosion, as the deactivation of biochar mainly results from the carbon oxidation which impairs the reducibility, blocks the pore, and changes the surface chemistry of carbon domain (Wu et al., 2020).

In summary, biochar engineered with controlled types and amounts of N-dopants could be generated to meet the different practical demands of various environmental applications.

Stoichiometric proportion of electroactive N-dopants and the customisation of their yield and density in N-doped biochar need to be further elaborated. Due to the different thermal stability of various N-dopants, the peak temperature is the critical factor that determines their yield and diversity in the resultant catalysts, designated as essential operational parameters in **Table 1**.

3. Fabrication of N-doped biochar

The N-doping techniques can be roughly categorised into two general types by different N sources, *i.e.*, internal N source within biomass and external N source with additives or purging ammonia. Based on the specific doping operation in practical fabrication, the doping style could also be divided into *in-situ* doping and post-doping. Their difference consists in the participating timing of N source, where *in-situ* doping and post-doping are correlated with the raw biomass and the already prepared biochar to be mixed with N source for thermal treatment, respectively.

3.1. N-doping with endogenous N contents in biomass

The critical point for the self-doping of N into biochar relies on the selection of biomass. This specified biomass should contain a large fraction of raw N contents within its overall chemical components or inherent macromolecular structure. Biological substances like algae, microorganisms, tissues, and other N-rich biowastes are more suitable to guarantee a high total N level in resultant biochar.

For instance, Liang et al. (2018) chose water hyacinth, which is ubiquitous in eutrophic aquatic ecosystems with outstanding N intake capacity, to produce an N-doped biochar cathode. The biochar electrode was prepared by integrating 80 *wt.*% water hyacinth-derived biochar powder (pyrolyzed at 800 °C), 10 *wt.*% acetylene black, and 10 *wt.*% polytetrafluoroethylene (PTFE) onto titanium mesh under vacuum and dried at 100 °C for 2 h. The as-prepared N-doped biochar

electrode was claimed to possess ultrahigh N content (7.71 *at.%*) compared with those in other reported biochars (2-7 *at.%*) (Shao et al., 2016). Accordingly, it exhibited excellent electrochemical properties due to the introduced N-dopants, *i.e.*, pyridinic-N (43.2%) and graphitic-N (56.8%). Another hydrophyte *agustifolia* was adopted by Ling et al. (2017) to produce self-doped biochar at 600 °C. The formed pyridinic N and pyrrolic N on biochar were found to possess an unpaired electron with high reactivity.

Apart from the biological substances from aquatic ecosystems, banana peel was also adopted to dope N into biochar by its endogenous N contents simultaneously. Specifically, Rong et al. (2019) squeezed banana peels into a slurry state to reach homogeneity of raw feedstock. Then, a hydrothermal treatment (180 °C, 6 h) coupled with subsequent calcination (600 °C, 2 h) was sequentially proceeded to carbonize the feedstock. The contained N-dopants involved various categories, *i.e.*, pyridinic N (28.5%), pyrrolic N (21.4%), and graphitic N (50.5%), due to the relatively low thermal treating temperature, while only the pyridinic N and graphitic N were proven effective in the catalytic activation.

Protein-rich biological substances are potentially suitable for the preparation of N-doped biochar. Ho et al. (2019) fabricated a series of N-doped graphitic biochars from C-phycocyanin extracted *Spirulina* residue, which is an N-rich cyanobacterium commonly applied in food science and medicine industry. Peak temperatures, including 400, 700, and 900 °C were employed to tune the types and density of N-dopants on biochar. An ultrahigh temperature over 900 °C was found to effectively diminish unwanted N-dopants to reach higher graphitic N proportion (14.7%). The as-prepared N-doped graphitic biochar exhibited higher graphitic degree and better conductivity, which accounted for its superior catalysis in the environmental decontamination. Similarly, Ma et al. (2019) employed human hair tissue as concomitant carbon and N sources to generate N-doped

biochar. The large fraction of incorporated pyrrolic N (58.5%) and graphitic N (41.5%) helped to achieve a useful function in circulating electron flow inside the biochar matrix. Xie et al. (2020) utilized a natural N-rich yeast (*Candida utilis*) to generate biochar nanosheets at 600 °C. This work abandoned the strategy to reach a highly graphitized carbon matrix and demonstrated that N-doped biochar with a low graphitization degree also showed outstanding catalysis.

It is worth noting that the biochars derived from C-phycocyanin extracted *Spirulina* residue, human hair, and *Candida utilis* all indicated a distinct non-radical activation of peroxides in comparison to the conventional radical-dominated pathway (Liu et al., 2019a; Yu et al., 2019a). This phenomenon was ascribed to the disrupted electronic feature of carbon framework owing to the accommodation of abundant graphitic N. Besides, Yu et al. (2019a) employed municipal sludge which was rich in N content due to the existence of endogenous polyacrylamide to fabricate magnetic N-doped biochar under pyrolysis at 900 °C. The self-doped N dopants, especially pyridinic N (27.2%) and graphitic N (64.2%), contributed *p*-electrons to the graphitic carbon to increase its catalytic capability (Luo et al., 2019; Oh et al., 2018).

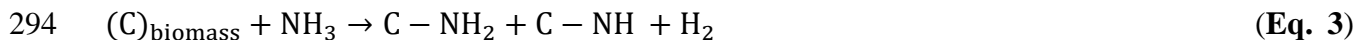
3.2. N-doping with external N precursors

For the N-doping with exogenous nitrogen sources, the commonly adopted N additives incorporate inorganic species (*e.g.*, ammonia, ammonium salts, and nitric acid) and organic species (*e.g.*, urea, melamine, and aniline). In contrast to the endogenous N-doping, the addition or impregnation of exterior N-rich substances target to construct an artificial nitrogenous ambient environment (Lin et al., 2012; Wang et al., 2019a; Zhu et al., 2018). Thus, the operational conditions might need to meet more strict and specific requirements. Upon the activation using different N sources with distinct macromolecular structures and chemical compositions, the type of the introduced N bonding configurations in resultant biochar also varied under various

operational conditions. It is worth noting that the abundance of oxygen-functional groups in biomass demonstrates a positive correlation with the N-doping level in resultant biochar, as oxygen functionalities can either directly bond with N precursor or undergo thermal decomposition to react with N precursor (Duan et al., 2018).

3.2.1. Ammonia purging

Ammonia purging could provide NH_3 molecules to react with the carbon framework during biomass thermal reforming, while their reaction intensity is relatively low and requires high-temperature environment. Besides, the ammonia activation often occurs on the interfacial solid-gas surface and leads to incomplete N-doping (*i.e.*, aminated contents) (Hou et al., 2019; Wu et al., 2020). For instance, Mian et al. (2018) adopted NH_3 ambient pyrolysis to reach the transformation of agar powder into N-rich biochar. The biochar precursor solids were pyrolyzed in a tubular reactor with temperature progressively ramping to the desired peak temperature (800 °C) under Ar environment (300 mL min⁻¹). Then, the Ar gas purging was promptly switched to ammonia purging (28%, 500 mL min⁻¹) until the cooling-down stage. The possible formation mechanism of attached N contents was then tentatively proposed, where the adequate -OH groups in agar powder played the critical role by reacting with NH_3 molecules to produce amino groups (R-NH_2) at high temperature (**Eq. 1**). The introduced amino groups further reacted with -OH to generate -C=N (**Eq. 2**). Another possible pathway (**Eq. 3**) was described by Chen et al. (2016), as NH_3 was regarded to react with carbonyl groups on biochar through the Maillard reaction accompanied by H_2 production. Carboxyl groups were also considered to form hydrogen bonding with NH_3 to promote N-doping and subsequently converted into pyridinic N and graphitic N (Jin et al., 2020). Accordingly, ammonia purging was conducive to developing the microporous structure with the consumption of oxygen functionalities (Yu et al., 2018).



295 Similar preparation protocol was employed by Yu et al. (2018) and Lian et al. (2016) to produce
 296 N-doped biochar derived from corn straw. The decoupled purging stages were exploited with three
 297 sections at different holding temperatures, namely (a) N₂ ambient pyrolysis at 600 °C for 2 h for
 298 biomass carbonization; (b) NH₃ ambient pyrolysis at 600 °C for 2 h to introduce N contents; and
 299 (c) NH₃ ambient pyrolysis at 600, 700, and 800 °C for 1, 2, and 3 h to tailor the types and amounts
 300 of N-dopants, respectively. The oxynitride was found to form at a lower peak temperature and a
 301 shorter holding time (600 and 700 °C for 1 h), further confirming that the activation reaction
 302 initiated from the reaction between oxygen functionalities and NH₃ molecules. Pyridinic N or
 303 pyrrolic N was transformed into graphitic N with the increase of peak temperature and retention
 304 time, indicating the feasibility of tailoring N-dopants by controlling operational conditions. The
 305 illustrative doping process is depicted in **Fig. 1**. As shown in **Table 1**, a high temperature over
 306 800 °C is more suitable to consolidate N atoms into the biochar framework. Overall, the plausible
 307 formation of graphitic N by ammonia purging was initiated at the surface functionalities through
 308 the sequential transformation of pyrrolic N to pyridinic N, and finally to the terminal graphitic N.

309 **3.2.2. Ammonium salts**

310 Zhu et al. (2018) fabricated N-doped graphitic biochar using a wetland plant (reed) as biochar
 311 precursor and ammonium nitrate (NH₄NO₃) as N source. As indicated in **Fig. 2a**, the pulverized
 312 reed powder was immersed and agitated in 50 mL ethanol containing 1 g ammonium nitrate to
 313 achieve the homogenous dispersion of N source over biomass. After implementing the solvent
 314 evaporation at 85 °C, the obtained mixed slurry was annealed at 900 °C to produce N-doped

biochar with high graphitic N ratio (61.7 *at.%* of the total N content). The employed ammonium salt seemed to act as both a pore-forming structural modifier and a reductive N-doping agent because it simultaneously releases NH₃, N₂, or N₂O during the thermal decomposition. A similar conclusion was proposed by Zhou et al. (2018) in the preparation of N-doped biochar using N-containing phosphates. The added salts mainly decomposed into NH₃ modify the carbon surface during pyrolysis. It can be assumed that the mechanistic formation route of N-dopants using ammonium salts is similar to that using ammonia purging, whereby the NH₃ molecules first combine with defective sites terminated with oxygen functionalities and subsequently are converted to respective N-dopants.

3.2.3. Organic additives

N-doping using organic additive is a handy one-pot method to obtain N-doped biochar, as it only requires the homogenous mixing of biomass and organic additive. The subsequent preparation procedure can follow that of conventional biochar production, which makes it more accessible for scientific communities.

Amongst all organic nitrogen additives, urea is a ubiquitous representative as it contains both carbon and N elements, which is conducive to the introduction of alien N atoms into carbon matrix *via* co-polymerization of biomass and N source. As shown in **Fig. S1a**, Oh et al. (2018) adopted lignocellulosic spent coffee grounds mixed with urea to fabricate N-doped biochar. The preparation procedure consisted of simple mixing by agate mortar and subsequent, direct pyrolysis, and the weight ratio of biomass to urea and peak temperature was set at 1:5 and 1000 °C, respectively. This simple procedure avoided the complicated gas purging and post-treatments to remove salt depositions. Impregnation of urea on biomass is another available approach to reach homogeneity of feedstocks. Ding et al. (2020) immersed 2 g rice straw into 80 mL water containing

0.75 g dissolved urea. After solvent evaporation, the mixed slurry was transferred to a tubular reactor for pyrolysis at 1000 °C. The weight ratio between biomass and N source was 2:0.75. Compared with dry mixing, the impregnation can reduce the N source dosage irrespective of an additional solvent evaporation process.

The N-doped biochar related to urea activation generally reported the ultrahigh SSA due to the decomposition of urea within the biomass. This phenomenon might result from the thermal instability of mixed urea to release NH₃ to open up pores. Wang et al. (2019b) also claimed the radicals might be formed during the decomposition of urea at high temperatures and corrode biomass to reach a richer porosity. Chen et al. (2019) considered urea might act as an expansion-reduction agent to cause more reduction and exfoliation during the preparation of reduced GO, which coincided with the phenomenon reported in N-doped biochar fabrication.

For operational conditions using organic additives, the reaction temperature should be carefully controlled as the N-rich sources such as urea and melamine tend to decompose into different intermediate products under specified peak temperature. Oh et al. (2018) claimed that the urea would undergo polycondensation to generate intermediate products including cyanuric acid and melamine. Carbon nitride would be formed during the initial pyrolytic stage at 300 °C with the appearance of various aminated moieties (*i.e.*, -NH₂, N-H, and C-N) on biochar surface. When the temperature was elevated to above 400 °C, these N-based moieties could be decomposed and coalesced into carbonized biomass lattice to form various N-doped bonding configurations (*i.e.*, pyridinic N, pyrolytic N, and graphitic N). As temperature further increased to above 700 °C, only a large fraction of graphitic N could be preserved. Besides, urea could not diffuse into biomass internal macrostructure (Zaeni et al., 2020), suggesting that preliminary controlling the particle size of the feedstock may favour introduction of more N contents.

Similarly, melamine decomposition also follows decoupled stages with different intermediates. An inert product, such as C_3N_4 , would be primarily generated in a lower pyrolytic temperature ($< 600\text{ }^{\circ}\text{C}$), and only a minor amount of melamine could be incorporated to form N-dopants (Wang et al., 2019c). A higher temperature over $700\text{ }^{\circ}\text{C}$ could help to consolidate N-dopants and to develop a graphitic lattice. Although most organic additives require different temperatures to decompose, the type of N-dopants tends to follow a distinctive order with $700\text{--}800\text{ }^{\circ}\text{C}$ as the borderline (as shown in **Table 1**), *i.e.*, pyridinic N and pyrrolic N dominate when peak temperature is lower than $700\text{ }^{\circ}\text{C}$ and graphitic N governs at a higher temperature over $800\text{ }^{\circ}\text{C}$. Holding time marginally influences the compositions of N bonding configurations, which are different from ammonia purging or ammonium salts activation (Oh et al., 2018). This suggests that the organic additives would coalesce N atoms into carbon lattice *via* co-polymerization, different from the carbon surface interaction with NH_3 molecules.

3.3.Co-doping technologies

Although sole doping of sulphur (S), boron (B), phosphorus (P), or iodine (I) into carbon matrix was reported to be ineffective for carbon-based catalysis (Duan et al., 2015c), tailoring the physicochemical properties of N-doped biochar by co-doping another foreign atom into a carbon matrix is triggering attention, as this technique might increase the reactivity of N-doped biochar by introducing synergistic bonding configurations. Due to the different electrochemical properties of each alien atoms in terms of their atomic radius and orbitals, electronegativities, and electron density, the electronic and spin nature of N-doped biochar could be further tailored.

As shown in **Fig. 3a-d**, Ma et al. (2019) found the slight co-doping of S contents ($1.04\text{ at.}\%$) in the N-doped biochar derived from human hair notably enhanced its electrochemical carbocatalysis. The doped sulphur contents mainly consisted of thiophene S on the edge sites rather than inert

oxygenated S. Considering the close electronegativity between carbon and S atoms (Pauling scale: $\chi_s = 2.58$ vs. $\chi_c = 2.55$), the coalesced S atoms might cause a distinct spin-dominated activation to reach a spin disruption in comparison to the charge-dominated regime from sole N activation (Ortiz-Medina et al., 2019). The positive role of S to synergize with doped N atoms in the carbocatalysis was also reported on other carbonaceous materials like graphene (Duan et al., 2015d; Liang et al., 2012). Nevertheless, Ding et al. (2020) claimed the S doping negatively influenced the catalytic capacities of N-doped biochar, indicating that the co-doping technique on biochar is still in its embryonic stage and need further elucidation.

Boron is another earth-abundant element applied in the heteroatoms doping technique. Chen et al. (2019) successfully doped N and B on a simplified carbon platform, *i.e.*, graphene, to manufacture a highly efficient catalyst. The substituted B atoms in graphitic carbon structure were capable of promoting graphitization degree and suppressing oxidative corrosion. The bonding configurations among C, N, and B were vital to determine the reactivity of resultant composite, as B can easily neutralize the unpaired electron of N-dopants to cause an electron-deficient region (Zhao et al., 2013). The B-C-N heteroring was considered to be most reactive, especially when B atoms were in the meta position of N atoms. In contrast, hexagonal boron nitride appeared to be chemically inert and inhibited carbocatalysis (Ma et al., 2011). No relevant biochar research reported the co-doping of N and B, which might result from that inherent complexity and vague interpretation.

Apart from non-carbon heteroatoms doping, metal atoms with dense electron population were also involved in this co-doping scheme. Different from conventional metal incorporation, the co-doped metal atoms need to maintain the metallic state by Me-N-C or Me-O-C bonding configurations to give rise to the electrochemical state in the interactive region. Zhong et al. (2020)

successfully fabricated N-Cu co-doped biochar, and the Cu atoms were auto-reduced by biomass when calcinated under the inert gas environment. However, it remains inconclusive whether metal could be regarded as heteroatoms irrespective of their high electroactive efficacy.

3.4. Emerging fabrication methods

Apart from traditional pyrolysis, several emerging processing methods have been developed to produce N-doped biochar. Hydrothermal carbonization process can be conducted at a relatively low temperature (*i.e.*, 160–300 °C) and an autogenic high pressure (*i.e.*, 200–600 bar). During the ionic reaction between biomass and water-induced ions (*i.e.*, hydronium and hydroxide ions) under subcritical conditions (Sevilla and Fuertes, 2009), the addition of N-containing contents might lead to the successful doping. Nevertheless, the primary dopants derived from hydrothermal carbonization are barely elaborated at the present stage. Besides, a thermochemical microwave method was also applied to enhance the N-doping, and the main dopant was found to be pyridinic N (12.9–15.7%), pyrrolic N (45.6–58.3%), and graphitic N (28.7–38.6%) (Wang et al., 2018a). Wan et al. (2020b) also found that microwave-assisting ammonia purging led to the primary edge-nitrogenation of pyridinic N (11.5%) and pyrrolic N (42.9%) on cellulose-derived biochar. The mechanochemical ball-milling process was adopted to introduce nitrogenous contents onto biochar (Xu et al., 2019b). The kinetic energy of moving balls potentially broke the inert carbon structure and incorporated a certain amount of N functionalities. At the same time, the energy appeared too weak to convert surface nitrogenous functionalities into N-dopants. Overall, these techniques can significantly reduce the energy input, which might trigger new strategies for facile N-doping. The relevant research is still scarce and much needed.

3.5. Limitations of different N-doping methods

Under different practical purposes, the specified operational procedure could be selected to

reach the desired N-dopants for the expected demand. Compared with post-doping treatment, the *in-situ* doping is more effective in incorporating N into carbon lattice, because N source can experience the integral carbon reforming processes during the biomass pyrolysis, *i.e.*, dehydration, decarboxylation, condensation, repolymerization, and aromatization (Sun et al., 2014). Accordingly, the occurrence of N content coalesce into re-united hexagonal rings is facilitated. In contrast, the already prepared biochar, especially the highly graphitized ones prepared under high temperature ($> 700\text{ }^{\circ}\text{C}$), is well-ordered and tends to demonstrate inert and stable features resisting alien atom doping. As a consequence, the N-doping style for those under the post-doping procedure is generally limited to the edge-nitrogenated types (*i.e.*, pyrrolic N and pyridinic N) bound onto biochar surface.

Apparently, the self-doping technique avoids the addition of toxic or costly chemicals (Gao et al., 2016). It tightly matches with the sustainable and green feature of biochar production without the involvement of extra energy or chemical inputs. Thus, its practical significance is recommended to be highlighted in future work. Considering that the N contents are well-acknowledged to be thermally unstable until combined into intact hexagonal carbon units, the endogenous self-doping is energetically preferential to fix nitrogen contents and mitigate their release into the atmosphere. Furthermore, the biomass wastes requiring disposal are abundantly available worldwide and vary in chemical compositions. More attention should be paid on the selection of proper biomass and its low-cost transformation into heteroatoms self-doped catalysts in the future.

To assure more introduced N-dopants, a continuous ammonia purging flow or a tightly sealed reactor is usually a necessity, which significantly increases the operational difficulties and impedes the up-scaling application. The employment of inorganic N sources can cause a deposition of

inorganic salts to form a monolayer dispersed on the surface of resultant biochar (Ho et al., 2019; Xu et al., 2020). The interaction between biomass and impregnated N-containing substances is usually a single-layer process that preferentially takes place on the carbon surface, leading to a reduced SSA and a blocked porous structure. Post-treatment methods such as pickling or acid washing are available to alleviate this issue. However, this complicated preparation procedure is not industrially and economically attractive. Thus, the N-doping using ammonium salts is recommended to coordinate with other techniques that require similar post-treatment such as molten salt activation (*e.g.*, ZnCl_2) to reach simultaneous surface cleaning.

N-doping using organic additives seems to be facile, economical, and controllable compared with the aforementioned methods. The resultant N-dopants can also be tuned under different peak temperatures to meet specified practical demand. Nevertheless, the adoption of organic sources such as urea will ineluctably release greenhouse gas (*i.e.*, NO_x) due to the incomplete combustion of feedstocks. This would exert long-term detrimental global effects from the life cycle perspective. In the future study, the optimization between practical significance and environmental concern is recommended to be further analyzed.

4. N-doped biochar for different applications

With the tuned intrinsic properties (*e.g.*, surface chemistry, graphitization degree, and defective level) and extrinsic properties (*e.g.*, SSA, porosity, and morphology) owing to the introduced N-dopants, N-doped biochar with superior capability has been applied in various fields mainly involving adsorption, catalytic remediation, and energy conversion and storage.

4.1. Adsorption of pollutants

Adsorption is a conventional process to reach phase separation of pollutants from its original

medium to remediate environmental contamination in air or soil or aqueous solution. Biochar adsorption mechanisms for organic pollutants mainly involves electrostatic force, hydrogen bonding, pore-filling adsorption/partition, π - π interaction, and hydrophobic interaction (Sun et al., 2019), while its adsorptive performance towards metal/metalloids is governed by ion exchange, cation- π bonding, metal-ligand complexation with surface oxygen functionalities, and co-precipitation with endogenous mineral contents (Sun et al., 2020; Zhong et al., 2019a).

It is generally known that the adsorption capability of biochar is highly correlated with the type of precursor feedstock. For instance, biochar prepared from biowastes with high ash contents (*e.g.*, animal manure and sewage sludge) are more efficient in removing metal/metalloids due to the high cation exchangeability, but inert towards organics. Overall, the adsorption efficiency of raw biochar is still limited without further physical/chemical modification. The scientific community is, therefore, particularly interested in fabricating biochar that could target a broad spectrum of pollutants to increase its practical applications. The emergence of N-doping is regarded as a potential game-changer, as it can introduce N-dopants to improve both the basicity of carbon surface to facilitate the electrostatic interaction and the textural characteristics of biochar to provide more interactive region.

4.1.1. Adsorption of metals and metalloids

Metals and metalloids usually undergo interspecies conversion when ambient pH changes. Thus, the electroactive contents on the interfacial carbon surface play a vital role in the removal of metals and metalloids. The introduction of various N-dopants, known as typical basic sites, could readily provide unpaired electrons to accommodate metal cations onto biochar surface. As indicated in **Table 3**, the best adsorption performance of various N-doped biochars was found to take place below neutral pH values, because the protonation of introduced N-dopants in the acidic

environment could help to attract more metal cations. As shown in **Fig. S2**, an agar derived biochar activated by NH_3 (ABF-N₈₀₀) achieved a high Cr(VI) adsorption capacity of 142.9 mg g⁻¹ via enhanced electrostatic interaction attributed to the introduced nitrogenous contents (Mian et al., 2018).

N-dopants can also enhance the hydrophilicity of the biochar surface to facilitate the contact with metal ions in solution and coordinate with metals and metalloids to form a chemical complexation. Yu et al. (2018) reported the excellent adsorption performance of N-doped biochar derived from crop straw towards both Cu(II) (1.63 mmol g⁻¹) and Cd(II) (1.76 mmol g⁻¹), and the adsorptive mechanism was mainly ascribed to surface complexation with graphitic N and surface hydroxyl groups. Ling et al. (2017) fabricated N-doped biochar derived from hydrophyte to stabilize Pb(II) with an ultrahigh removal efficiency of 893 mg g⁻¹, and the surface coordination by pyridinic N, pyrolytic N, and C=O was regarded as the adsorptive mechanism.

Biochar produced via hydrothermal carbonization with a higher surface electron population was also reported to exhibit favourable affinity towards heavy metals. Guo et al. (2019) investigated the effect of peak temperature on the adsorption capacities, and selectivity of *Camellia sinensis* derived N-doped biochar. Biochar produced at 240 °C (HTC-240) was found to show the highest adsorption performance toward Cu(II), Pb(II), and Cr(VI) with adsorption capacities at 44.0, 83.9, and 94.7 mg g⁻¹, respectively. High-temperature biochar (HTC-280) exhibited a higher adsorption affinity towards Zn(II) with an adsorption capacity of 64.8 mg g⁻¹. Despite the chemical complexation, several other mechanisms involving mass transfer, intraparticle diffusion, and chemisorption also participated due to the modified extrinsic properties during N-doping. Similarly, Gai et al. (2016) utilized endogenous N contents in a microalgae (*Chlorella pyrenoidosa*) to modify rice husk-derived biochar via hydrothermal carbonization. The prepared N-doped

biochar showed an increased Cu(II) adsorption capacity to 29.1 mg g⁻¹ compared with 13.1 mg g⁻¹ of raw biochar. The adsorption mechanism was governed by surface complexation rather than electrostatic attraction.

4.1.2. Adsorption of organics

Compared with metals and metalloids, organics are more nucleophilic due to their electron-rich macromolecular compositions. Accordingly, the evolved π - π electron donor-acceptor interaction and Lewis acid-base interaction by N-dopants on N-doped biochar dictate the adsorption of organic pollutants. Besides, the introduction of N-dopants can cause electron redistribution by polarizing π electron from carbon layers and create positive holes, which may show a strong affinity with electron-rich aromatic rings (Wang et al., 2018a). As illustrated in **Fig. S3**, Yang et al. (2017) fabricated a wheat straw derived N-doped biochar sheet for atrazine removal. The adsorption capacity reached 82.8 mg g⁻¹ and the principal mechanism originated from π - π electron donor-acceptor interaction between atrazine molecules and electron-deficient carbon region. Li et al. (2019a) synthesized a corn stalk derived N-doped biochar and reached enhanced phenol adsorption ability at 95.9 mg g⁻¹. Both Lewis acid-base interaction and electron donor-acceptor interaction contributed to the removal of phenol. These interactions were also considered to account for the removal of dyes, *i.e.*, acid orange 7 and methyl blue with removal capacities of 292 and 436 mg g⁻¹, respectively, by corn straw derived N-doped biochar (Lian et al., 2016). Lu et al. reported (2017) the increased basicity of N-doped biochar could enhance its affinity towards acidic pollutants (bisphenol A, 9.68 mg g⁻¹).

Besides, N-doped biochar has been applied in the adsorption of gaseous pollutants, *e.g.*, toluene and CO₂, as basic N-doped biochar surface can facilitate its adsorptive behaviour towards nonpolar or weakly polar gaseous substances due to electron pair donation (Jin et al., 2020; Wang et al.,

2019b). The increased basicity from introduced pyridinic N and pyrrolic N significantly increased the adsorption capabilities of various N-doped biochars (AP-900, 496.2 mg g⁻¹; UP-900, 364.1 mg g⁻¹; APP-900, 444.9 mg g⁻¹) towards toluene (Zhou et al., 2018), which was consistent with that reported in CO₂ sequestration (AMBC, 10.15 mmol g⁻¹) by N-doped biochar beads (Nguyen and Lee, 2016).

4.2. Advanced oxidation processes

Compared with pollutant adsorption, advanced oxidation processes (AOPs) have the potential to reach complete mineralization of organics by the use of catalysts and oxidizing agents (e.g., peroxides and ozone) under appropriate reaction conditions. Since the emergence of persulfate-based AOPs as a robust system to *in-situ* degrade organic contaminants in soil and groundwater, a myriad of carbonaceous materials has been widely applied as metal-free peroxide activators (Wang et al., 2020). Crystalline nanocarbons, including graphene and CNTs, are most frequently studied owing to their superior electrochemical properties (*i.e.*, lower internal resistance and energy barrier) (Duan et al., 2015e). Biochar-based materials were not considered until recent years due to their structural complexity (*i.e.*, high amorphous content) and nonstoichiometric nature (*i.e.*, inferior doping efficiency and weaker electrocatalysis).

In environmental decontamination, the common active sites on engineered biochar are electron-rich structures, such as inherent functionalities, environmental persistent free radicals (EPFRs), and incorporated metal centers. Nevertheless, the conventional redox-active features are found to be easily consumable and prone to be irreversibly oxidized after reaction (Li et al., 2020). It is also generally deemed that the EFPRs and metal contents can induce uncontrollable environmental implications of great human health concern when released into the ecosystem (Pan et al., 2019; Ruan et al., 2019). In contrast, the N-dopants are regarded as environmentally friendly and cost-

effective as the concerned synthesis protocols and feedstocks are recognized to be green and abundantly available, which falls into the concept of bioresource recycling scope consistent with biochar production. The unveiling of graphitic biochar fabricated under high temperature ($> 700\text{ }^{\circ}\text{C}$) effectively broadened the application of biochar, as unproductive amorphous carbon contents can be converted to graphitic basal plane and N-dopants are readily consolidated into carbon lattice under specific thermal conditions. In the meantime, the unique properties of biochar, such as high oxygen contents and structural defects, can be reciprocally leveraged to promote the accommodation of N atoms into carbon lattice.

It is well accepted that pyridinic N and graphitic N are more desired in catalytic reactions (Xie et al., 2020). As aforementioned, the introduction of pyridinic N and graphitic N onto biochar could disrupt the electronic properties of the original biochar framework. As depicted in **Fig. 4**, pyridinic N possesses unpaired electrons that can serve as confined radicals to directly capture the peroxide molecules with high electrophilic feature (Duan et al., 2016; Duan et al., 2018), while graphitic N with *n*-type conduction increases the overall reactivity of localized carbon region towards electron-acceptor oxyanions (Zaeni et al., 2020). Owing to the different electronegativity between N and C atoms, the peroxide molecules could be adsorbed on positively charged adjacent C atoms and then accept the electrons delivered from N centers. In the presence of N-dopants, this integrated adsorption-activation process can lower the energy threshold of the peroxide O–O bond required to be dissociated/cleaved (Duan et al., 2018).

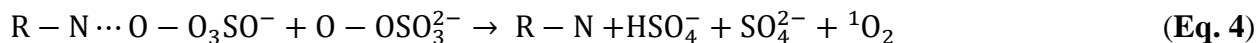
Intriguingly, mild and sustainable catalysis (*i.e.*, singlet oxygenation or direct electron transfer) is ubiquitous in peroxide activation using N-doped biochar, which follows a fascinating non-radical mechanism distinct from those conventional radical-based oxidation processes. This process is a carbon/peroxide interfacial process rather than that releases radicals into the bulk

591 solution. Accordingly, milder and sustainable mechanisms can be delivered to avoid the
592 shortcomings from non-selective radicals that might lead to the irreversible carbon surface
593 oxidative erosion or the generation of highly halogenated products, promising better recyclability
594 and sustainable operational potential of biochar. Furthermore, non-radical catalytic reaction pauses
595 when pollutant molecules are depleted, and chemical input can be reduced by preserving excessive
596 peroxide molecules for future use (Oh and Lim, 2019). In this regard, increasing attention are being
597 paid to this metal-free technology to fabricate more efficient carbocatalysts.

598 Since graphitic N-doped biochar (N-BC900, **Fig. 2**) was first fabricated at ultrahigh temperature
599 (900 °C) to activate PDS molecules for the degradation of various organics (*e.g.*, orange G), the
600 well-ordered biochar structure was found to possess high adsorption affinity towards both PDS
601 and organic molecules to provide an ideal carbon substrate with high conductivity for
602 electrochemical interactions (Zhu et al., 2018). The excellent electroactive interface of N-doped
603 biochar subsequently triggered an integral $^1\text{O}_2$ and electron transfer regime (surface-confined
604 activated metastable complex) to degrade organics *via* a non-radical pathway. A similar
605 phenomenon was elaborated in the PMS system activated by N-doped biochar derived from
606 lignocellulosic biowaste for bisphenol A degradation in **Fig. S1d** (Oh et al., 2018). Compared with
607 the symmetric PDS molecules ($^-\text{O}_3\text{SO}-\text{OSO}_3^-$), PMS ($\text{HO}-\text{OSO}_3^-$) is more susceptible to
608 electrophilic attack due to its longer peroxide O–O bond ($l_{\text{O-O}}=1.453 \text{ \AA}$) and unstable asymmetric
609 structure (Wu et al., 2020).

610 The correlation between N bonding configuration and catalytic stability was unveiled, whereby
611 graphitic N manifested higher catalytic activity and stability in contrast to pyridinic N and pyrrolic
612 N. The recovery of graphitic N from pyridinic N could be achieved by implementing high-
613 temperature annealing (*i.e.*, 800–1000 °C) at the expense of overall N level. The generation of $^1\text{O}_2$

in the peroxide activation was supported by several studies on other N-doped biochars (Ding et al., 2020; Ma et al., 2019; Wan et al., 2020b), as graphitic N could confine PDS/PMS molecules as metastable complex to prompt the self-decomposition of peroxide molecules (**Eq. 4**). Besides, the formed surface-confined complex can follow another electron transfer regime to directly oxidize co-adsorbed organic pollutants (Ho et al., 2019). Specifically, the electrons delivered from co-adsorbed electron-rich organics could transport through highly graphitized sp^2 -hybridized carbon framework to the activated oxyanion/carbon complex with the difference of their inherent redox potentials as a driving force. This phenomenon is frequently reported in heteroatoms-doped nanocarbons (Duan et al., 2015f; Ortiz-Medina et al., 2019), which confirmed the critical role of conductive well-developed carbon π -electron network.



Although the formation of surface-confined complex on N-doped biochar is regarded as the initial step in non-radical peroxide activation, most studies found the catalytic degradation in AOPs should be a hybrid process consisting of both radical and non-radical pathways due to the inevitable participation of other electroactive components (Xie et al., 2020; Xu et al., 2020; Zaeni et al., 2020). Similarly, the participation of metals would increase the contributions of radical pathways in the degradation as transition metals energetically showed higher reactivity than non-metal atoms in the electrochemical process (Liu et al., 2019b; Rong et al., 2019; Zhong et al., 2020), while metal-free catalysis is always recommended as a prior choice owing to its environmentally benign feature. As shown in **Table 4**, the operational parameters (*e.g.*, catalyst loading, peroxide dosage, and pH) significantly influenced the reaction constant rate.

4.3. Energy storage and conversion

Global warming, environmental deterioration, and energy shortage in the current fossil fuel

society have led to an ecological crisis. The storage and conversion from renewable and abundant sources (*i.e.*, sun, wind, water, geothermal, and biomass) could be a rational option to relieve this issue. N-doped biochar materials have shown great potential in energy storage and conversion fields owing to their outstanding tunable surface chemistry and electrochemical properties. Typically, N-doped biochar as a prospect electrocatalyst also extended their applications in accomplishing electrochemical reduction (Yao et al., 2020), electrochemical detection (Liu et al., 2020), aqueous aluminium/air battery (Wang et al., 2015b), lithium-sulphur batteries (Li et al., 2019b), alkaline fuel cell (Borghei et al., 2017), and hydrogen evolution reaction (An et al., 2018; Zhou et al., 2015).

4.3.1. Oxygen electrocatalysts

Oxygen reduction reaction (ORR) is one of the most important reactions occurring in electrochemical energy storage and conversion processes, including fuel cell, water splitting, and metal-air batteries. Given that the efficiency of ORR is notably restricted by the sluggish reaction rate of oxygen species and high inner energy barrier, high-performance, and cost-effective catalysts are highly desired to meet the demands for up-scaling commercial applications. Conventional oxygen electrocatalysts using noble metal (*e.g.*, Pt, Pd, and Ru) show many demerits such as low abundance on earth, high cost in fabrication procedure, and reduced tolerance towards CO and methanol. Given that the initial oxygen adsorption or the electron transport to the adsorbed oxygen species is regarded as the rate-limiting step in ORR, N-doped biochar with a high density of active sites and excellent extrinsic properties emerges as a rational alternative in the development of ORR electrocatalyst.

As shown in **Fig. S4**, Liu et al. (2015a) fabricated an N self-doped electrocatalyst derived from water hyacinth for ORR. The onset potential was calculated to be +0.98 V *vs.* reversible hydrogen

electrode (RHE), which was even more positive than that of commercial Pt/C (+0.95 V). The superior electrochemical properties were attributed to the abundant pyridinic N and graphitic N, as the lone-pair electrons from N-dopants can help to activate carbon π electrons for better adsorption of oxygen molecules and lead to higher conductivity. Liang et al. (2018) also employed water hyacinth biowaste to produce N-doped biochar in the $2e^-$ ORR for the generation of hydrogen peroxide (H_2O_2). The yield of H_2O_2 and current efficiency could be elevated to 1.7 mmol L^{-1} and 81.2%, respectively, compared with the pristine biochar without N-dopants (1.1 mmol L^{-1} and 28.3%). It could be concluded that the introduced N-dopants on biochar can act as electroactive sites to promise faster electron migration. As shown in **Table 5**, several other N-doped biochars were reported to be remarkably effective for ORR in both acidic and alkaline environment. Most of them showed a comparable onset potential and half-wave potential to those of costly commercial 20 wt.% Pt/C. Furthermore, the N-doped biochar appeared to be more tolerable towards methanol with a higher longer-term stability compared with noble metal electrodes (Borghei et al., 2017; Chen et al., 2014; Liu et al., 2014).

Interestingly, the active sites on N-doped biochar electrocatalysts all indexed to pyridinic N and graphitic N. This phenomenon coincides with the conclusion drawn in previous parts, as pyridinic N and graphitic N are regarded to be electroactive sites with highest electrochemical reactivity in redox reactions. SSA is also a key parameter to determine the reactivity of electrocatalysts, which is conducive to the fast mass transfer and electron migration (Pan et al., 2014). The decomposition of various N precursors can result in higher SSA, uniform N-doping, and a well-developed porous structure, which intimately match with the desired characteristics of ORR electrocatalysts. Simultaneous incorporation of transition metal contents is another appealing strategy to obtain high-performance ORR catalysts. The participation of metal contents was found to catalyse the

formation of N-dopants apart from their direct contribution as Lewis basic sites in ORR (Pi et al., 2020; Zhang et al., 2017).

Oxygen evolution reaction (OER) is another electrocatalytic process for energy storage and conversion featured as a four-electron process associated with applications in water splitting and rechargeable metal-air batteries. Due to its sluggish nature from low reaction kinetics, the oxygen electrocatalyst with excellent electrochemical capacities is essential to accelerate the OER rate and reduce overpotential. Similar to ORR, N-doped biochar based electrocatalyst could be a suitable candidate to replace the conventional noble metal catalyst (*e.g.*, IrO₂ and RuO₂) in OER owing to its high catalytic activity and excellent stability (Liu et al., 2019c). As shown in **Fig. S5**, Wang et al. (2017) fabricated a biochar-based material derived from *Chlorella*, and the synthesized electrocatalyst showed high performance in both ORR and OER. Apart from the favourable ORR half-wave potential at 0.84 V, which transcended that of commercial 20 wt.% Pt/C (0.83 V), its OER overpotential at 10 mA cm⁻² was 23 mV, also lower than the reference electrode IrO₂/C in 1.0 M KOH solution. Such a bifunctional feature was attributed to the simultaneous enrichment of pyridinic N and graphitic N as predominant active sites in ORR and OER, respectively.

4.3.2. Microbial fuel cell

Different from ORR and OER that rely on external power to initiate the reaction, microbial fuel cells (MFCs) is another technology that converts the organic or inorganic contaminants into electrical energy through the spontaneous metabolism of microbes (Wang et al., 2018b). The selection of electrode material is crucial in MFCs as it greatly influences the biofilm formation, inner energy barrier/resistance, and enrichment of pollutant molecules, *etc.* Considering that MFCs are mainly designed for practical wastewater treatment, the ideal electrode material applied in MFCs should possess superior electrochemical properties with relatively low prices, and

meanwhile, is biocompatible, durable, and environmentally friendly under microbial stress. In this regard, sustainable N-doped biochar can be an excellent precursor for manufacturing of the cathodic electrode for MFCs.

Biochar derived from milling residue showed a peak power output at $532 \pm 18 \text{ mW m}^{-2}$ in MFC comparable to those assigned to AC and graphite granule at 674 ± 10 and $566 \pm 5 \text{ mW m}^{-2}$, respectively (Huggins et al., 2014). Furthermore, the material cost for biochar preparation ($0.051\text{--}0.381 \text{ US\$ g}^{-1}$) was nearly 90% lower than its carbon counterparts ($0.8\text{--}2.5 \text{ US\$ g}^{-1}$ for AC and $0.5\text{--}0.8 \text{ US\$ g}^{-1}$ for graphite granule). As mentioned above, the participation of N-doping could significantly enhance the electrochemical properties with a relatively low increase in reagent cost. As shown in **Fig. S6**, Zhong et al. (2019b) fabricated N-doped biochar derived from watermelon rind as a cathode material. The as-prepared N-doped biochar possessed a current density and charge transfer resistance of 0.19 mA cm^{-2} and 20.6Ω comparable to those of commercial Pt/C catalyst (0.20 mA cm^{-2} and 37.6Ω). Compared with graphitic biochar (146.7 mW m^{-2} , $0.0004 \text{ US\$ g}^{-1}$), the power density of N-doped biochar could reach 262.0 mW m^{-2} while the price only increased to $0.015 \text{ US\$ g}^{-1}$, which was economically superior to commercial Pt/C (512 mW m^{-2} , $33 \text{ US\$ g}^{-1}$) (Huggins et al., 2015).

Another N-doped biochar derived from cellulose paper with an ultra-high surface area of $1170.6 \text{ m}^2 \text{ g}^{-1}$ was applied in MFCs (Yue et al., 2015). The maximum power density in this N-doped biochar/MFC system reached $1041 \pm 90 \text{ mW m}^{-2}$, which was much higher than that of Pt/C-based MFC ($584 \pm 10 \text{ mW m}^{-2}$). Noteworthily, Liu et al. (2015b) found the co-doping of phosphate using ammonium phosphate as N/P source could achieve an ultrahigh maximum power density at $2293 \pm 50 \text{ mW m}^{-2}$ in the N, P-doped biochar MFC system, which might suggest the great potential for co-doping technology in MFCs. As shown in **Table 6**, the key N-dopants pointed to pyridinic N

and graphitic N, further confirming their critical role in electrochemical reactions.

4.3.3. Energy storage vessels

In principle, there is no fundamental difference among biochar, activated carbon, and carbon black, except that biochar surface is usually rich in functional groups. Since the establishment of geobattery theory, *i.e.*, quinone/hydroquinone pairs can undergo reversible functional interspecies conversion on carbonized matrix (Klүpfel et al., 2014; Sun et al., 2017), the potential of utilizing biochar to fabricate energy storage vessels is unveiled.

Supercapacitor offers a fascinating approach to store clean/renewable energy and stands out due to its high power density, efficient reversibility, and good recyclability (Miller and Simon, 2008). With the highly scalable surface chemistry by selecting specific biomass precursors, thermal conditions, and modification methods, biochar has been experimented to produce high energy density supercapacitor. Biswal et al. (2013) produced biochar by single-step pyrolysis of dead plant leaves with a high surface area of $\sim 1230 \text{ m}^2 \text{ g}^{-1}$. The synthesized biochar showed a respectable specific capacitance of 400 F g^{-1} and an energy density of 55 W h kg^{-1} at a current density of 0.5 A g^{-1} in acidic electrolyte. The enhanced energy storage efficiency was ascribed to the introduction of N-dopants into biochar. Li et al. (2012) synthesized a supercapacitor electrode material using chicken eggshell membranes, and excellent specific capacitances of 297 and 284 F g^{-1} could be achieved in both basic and acidic electrolytes, respectively. This favourable electrochemical capacity was because of the redox reactions between N-dopants and oxygen functionalities. Liu et al. (2016) fabricated a porous N-rich carbon from sugar cane bagasse and urea with 323 and 213 F g^{-1} at the discharge/charge current densities of 1 and 30 A g^{-1} , respectively. Abundant porosities were found to conduce ion buffering and accommodation while high N content could notably increase the pseudocapacitance.

In the view of chemistry, the pyridinic N or pyrrolic N adjacent to a quinone oxygen atom is regarded as primary N-dopants contributing to the supercapacitor capacitance (Hulicova-Jurcakova et al., 2009), while graphitic N can accelerate the electron migration and introduce pseudocapacitance *via* the interaction with protons in an acidic electrolyte (Lee et al., 2013). Similar to foregoing applications, the co-doping technology also demonstrated a combined effect from the co-existence of N and S to improve the specific capacitance and cycling performance of banana-derived biochar supercapacitor (Wang et al., 2014).

4.3.4. Biofuel production

The conversion of biomass or CO₂ to value-added chemical products is one of the emerging applications of biochar (Cao et al., 2019; Xiong et al., 2017), which could provide an alternative method to alleviate the energy shortage in the current fossil fuel society. Value-added chemical production involves a series of reactions initiating with the saccharification of glucans to glucose. Subsequently, the produced glucose can be isomerised to fructose, which can be further upgraded to useful platform chemicals, such as hydroxymethylfurfural (HMF) (Yu et al., 2016). Isomerisation of glucose to fructose relies on Lewis acid (electron pair acceptor) *via* catalytic routes through a hydride shift from C2 to C1 or a hydrogen transfer from O2 to O1 of glucose, respectively (Binder et al., 2010; Yu et al., 2019b). As shown in **Fig. 5**, Chen et al. (2018b) fabricated a useful biochar catalyst derived from spent coffee grounds with melamine for the isomerization of glucose to fructose. Fast glucose conversion (12%) and high selectivity to fructose (84%) could be reached at a moderate temperature of 120 °C within 20 min. The coffee-derived biochar was superior to conventional catalysts, including aqueous hydroxides and amines (50–80%) with comparable catalytic activity (~20 mol% conversion within 20 min). Pyridinic N was regarded as the main catalytic site owing to its localized lone pair and nucleophilic nature.

The methanation of CO₂ to produce CH₄ is receiving tremendous attention because it could reach the mitigation of greenhouse gas release and the generation of biogas simultaneously (Dreyer et al., 2017). The most commonly used active catalysts for methanation are noble metals (*e.g.*, Ru, Rh, Pt, and Pd). Although these metals are catalytically active, they must be deposited onto inert supports to avoid sintering and aggregation. The evolvement of N-doped biochar can provide an economical carbon substrate. The abundant basic N-dopants can effectively donate electrons through which catalyzing reduction reactions and suppressing the deactivation of metal centers caused by coke deposition (Roldán et al., 2017). Wang et al. (2019b) produced N-doped biochar derived from *Pinus Sylvestris* with urea as Ru support. The generated catalyst could achieve a high CO₂ conversion rate of 93.8% and a CH₄ selectivity of 99.7%. The basic N-dopants (mainly pyridinic N and pyrrolic N) could serve as an electron donor to promote the Ru incorporation and anchoring sites for CO₂ adsorption to enhance the conversion.

4.4.Limitations of N-doped biochar in environmental applications

N-doping technology gives a great boost to biochar for its high performances on contaminant adsorption and catalytic remediation; however, the ideal regeneration protocols are not well coordinated. The introduced N-dopants will establish an electron-paired bonding towards adsorbed organics with irreversible features (Oh and Lim, 2019). Zhang (2019) claimed that the activity can be partially recovered *via* simple annealing at 800 °C, while an annealing temperature higher than 800 °C to evaporate/carbonize adsorbates and oxidized contents would cause the decomposition of N active sites. Wan et al. (2020b) employed a low-temperature treatment (250 °C) to restore the catalytic capability of N-doped biochar while this strategy was limited to remove organics with low evaporation points. More emerging methods (*e.g.*, sonication, microwave) with lower energy input should be explored to restore the active region of N-doped biochar in future work.

Furthermore, the correlation between the density of N-dopants and electrocatalytic performance remains unclear, as many researchers claimed that no relation was found between total N level and electrochemical activity (Nagaiah et al., 2010; Oh et al., 2011). Based on the current state of knowledge, only organics with simple molecular structure, lower ionized potential (< 9.0 eV), and abundant electron-rich functionalities (*e.g.*, amino and hydroxy groups) could be decomposed *via* non-radical pathway (Duan et al., 2019; Hu et al., 2017). To meet specific practical demands, diversity of pollutant selection should be taken into consideration in the future study.

At the present stage, the research on heteroatoms co-doped biochar is still not sufficient to reach a comprehensive conclusion. More relevant studies are encouraged since co-doping technology has been proven effective on other carbon platforms (Duan et al., 2015d; Tian et al., 2016). Ding et al. (2020) manufactured several N-doped, S-doped, and N, S-doped biochars to verify the synergies between different non-carbon heteroatoms, and found only N-doping exerted positive effects on the catalytic capacities of resultant biochar. The co-doping technology on biochar-based electrocatalyst fabrication is also inadequately explored, although density functional theory (DFT) calculations verified that the co-doping of another non-carbon atom could further alter the electronic nature of carbon matrix to increase its catalytic activity (Zhou et al., 2015).

Besides, the combination between N-doped biochar and MFCs needs further elaboration from mechanistic aspects. Notably, the influences of basic N-dopants on the material compatibility, microbe acclimation, electron transfer mechanism, synergies between electrode adsorption and biofilm, and long-term stability are yet to be revealed and should be addressed in the future study. Also, future work should focus on the advantage of the easily tunable features of heteroatoms-doped biochar to fabricate high-performance supercapacitors with well-developed porosities, electrical conductivity, and excellent durability towards electrolyte.

5. Conclusion

In this review, recent advances in the fabrications and applications of N-doped biochar are summarised and discussed. Generally, the superior electrochemical properties, versatile porous structure, and higher surface area of N-doped biochar can be achieved by selecting specific doping techniques and controlling the operational conditions during production. The green and sustainable nature of the N-doping technique are in alignment with the biochar production with low environmental concern. The abundant electroactive N-dopants make N-doped biochar a promising alternative in various environmental applications such as adsorption, catalytic decontamination, energy storage, and biofuel production to replace the conventional metal-based catalysts. In particular, a comprehensive understanding of the doping mechanism and the characteristics of each N-dopants elaborated in this work propel the field of biochar to further apply this appealing material for more novel sustainable carbocatalysis in the future.

6. Perspectives

For directions of future study on N-doped biochar, several aspects can be further explored: (a) The importance of the self-doping technique should be highlighted in future N-doped biochar production. Combined with plant biotechnology, eutrophication mitigation, and biomass disposal can be simultaneously achieved by intaking heteroatoms precursor into biomass prior to carbonization as a sustainable method; (b) Rational manipulation of types and densities of N-dopants during production and applications should be explored and optimized, while the present studies lack the emphasis on the fate of N-dopants and their environmental implications; (c) The co-existing impurities that are unlikely to be removed entirely from biomass, especially

endogenous metal contents, will lead to nonnegligible effects on the physicochemical properties (*i.e.*, carbon structure, N-dopants, defective level, and graphitic degree) of resultant N-doped biochar. Relevant research could provide a systematic investigation on the influence of these impurities by selecting specific biomass or adding additives, and compare with other simplified carbonaceous material with similar carbon structure, *e.g.*, AC; (d) The full illustration of the doping mechanism remains a challenge. *In-situ* advanced characterization and computational modeling could help to construct a fundamental scheme. Considering the paramagnetic properties of N-dopants with unpaired electrons, combining the electron paramagnetic spectroscopic (EPR) characteristic signals and DFT calculations might be a promising approach to reveal the formation and compositions of N-dopants; (e) Metal-free carbonaceous materials usually exhibit lower stability when exposed to harsh conditions. The stability and efficiency of N-doped biochar should be optimized combined with the exploration of co-doping technology. The regeneration of spent N-doped biochar also requires more concentration; (f) Given the sustainable and economic features of N-doped biochar; future work could focus more on the non-radical degradation, biorefinery, and fabrication of energy storage devices to expand its role in green and sustainable chemistry. The current progress of N-doped biochar in environmental fields triggers inspiring accomplishment. With continuous contributions to promoting this material, up-scaling practical applications of N-doped biochar can give impetus to the value-added utilization of renewable bioresource.

Acknowledgment

The authors appreciate the financial support from the Hong Kong Research Grants Council (PolyU 15217818) and Hong Kong International Airport Environment Fund (Phase 2) for this study.

867

868 **References**

869 [1] J.S. Cha, S.H. Park, S.-C. Jung, C. Ryu, J.-K. Jeon, M.-C. Shin, Y.-K. Park, Production and
870 utilization of biochar: A review, *Journal of Industrial and Engineering Chemistry*, 40 (2016) 1-15.

871 [2] X. Xiong, I.K.M. Yu, L. Cao, D.C.W. Tsang, S. Zhang, Y.S. Ok, A review of biochar-based
872 catalysts for chemical synthesis, biofuel production, and pollution control, *Bioresource technology*,
873 246 (2017) 254-270.

874 [3] I. Anastopoulos, I. Pashalidis, A. Hosseini-Bandegharaei, D.A. Giannakoudakis, A. Robalds,
875 M. Usman, L.B. Escudero, Y. Zhou, J.C. Colmenares, A. Núñez-Delgado, É.C. Lima, Agricultural
876 biomass/waste as adsorbents for toxic metal decontamination of aqueous solutions, *Journal of*
877 *Molecular Liquids*, 295 (2019) 111684.

878 [4] A. Demirbaş, Mechanisms of liquefaction and pyrolysis reactions of biomass, *Energy*
879 *Conversion & Management*, 41 (2000) 633-646.

880 [5] J. Li, J. Dai, G. Liu, H. Zhang, Z. Gao, J. Fu, Y. He, Y. Huang, Biochar from microwave
881 pyrolysis of biomass: A review, *Biomass and Bioenergy*, 94 (2016) 228-244.

882 [6] D.-W. Cho, K. Yoon, Y. Ahn, Y. Sun, D.C.W. Tsang, D. Hou, Y.S. Ok, H. Song, Fabrication
883 and environmental applications of multifunctional mixed metal-biochar composites (MMBC)
884 from red mud and lignin wastes, *Journal of hazardous materials*, 374 (2019) 412-419.

885 [7] Q. Xu, Z. Chen, Z. Wu, F. Xu, D. Yang, Q. He, G. Li, Y. Chen, Novel lanthanum doped
886 biochars derived from lignocellulosic wastes for efficient phosphate removal and regeneration,
887 *Bioresource technology*, 289 (2019a) 121600.

888 [8] J. Lee, X. Yang, S.-H. Cho, J.-K. Kim, S.S. Lee, D.C.W. Tsang, Y.S. Ok, E.E. Kwon,
889 Pyrolysis process of agricultural waste using CO₂ for waste management, energy recovery, and

biochar fabrication, *Applied Energy*, 185 (2017a) 214-222.

[9] M. Tripathi, J.N. Sahu, P. Ganesan, Effect of process parameters on production of biochar from biomass waste through pyrolysis: A review, *Renewable & Sustainable Energy Reviews*, 55 (2016) 467-481.

[10] A.D. Igalavithana, S. Wan Choi, P.D. Dissanayake, J. Shang, C.-H. Wang, X. Yang, S. Kim, D.C.W. Tsang, K.B. Lee, Y.S. Ok, Gasification biochar from biowaste (food waste and wood waste) for effective CO₂ adsorption, *Journal of hazardous materials*, (2019) 121147.

[11] X. Yang, A. Tsibart, H. Nam, J. Hur, A. El-Naggar, F.M.G. Tack, C.-H. Wang, Y.H. Lee, D.C.W. Tsang, Y.S. Ok, Effect of gasification biochar application on soil quality: Trace metal behavior, microbial community, and soil dissolved organic matter, *Journal of hazardous materials*, 365 (2019a) 684-694.

[12] S. You, Y.S. Ok, S.S. Chen, D.C.W. Tsang, E.E. Kwon, J. Lee, C.-H. Wang, A critical review on sustainable biochar system through gasification: Energy and environmental applications, *Bioresource technology*, 246 (2017) 242-253.

[13] P. Gao, D. Yao, Y. Qian, S. Zhong, L. Zhang, G. Xue, H. Jia, Factors controlling the formation of persistent free radicals in hydrochar during hydrothermal conversion of rice straw, *Environmental Chemistry Letters*, 16 (2018) 1463-1468.

[14] J. Wang, S. Wang, Preparation, modification and environmental application of biochar: A review, *Journal of Cleaner Production*, 227 (2019) 1002-1022.

[15] D.-W. Cho, G. Kwon, K. Yoon, Y.F. Tsang, Y.S. Ok, E.E. Kwon, H. Song, Simultaneous production of syngas and magnetic biochar via pyrolysis of paper mill sludge using CO₂ as reaction medium, *Energy Conversion and Management*, 145 (2017) 1-9.

[16] M.-T. Yang, Y. Du, W.-C. Tong, A.C.K. Yip, K.-Y.A. Lin, Cobalt-impregnated biochar

produced from CO₂-mediated pyrolysis of Co/lignin as an enhanced catalyst for activating peroxymonosulfate to degrade acetaminophen, *Chemosphere*, 226 (2019b) 924-933.

[17] K.N. Palansooriya, Y.S. Ok, Y.M. Awad, S.S. Lee, J.-K. Sung, A. Koutsospyros, D.H. Moon, Impacts of biochar application on upland agriculture: A review, *Journal of environmental management*, 234 (2019) 52-64.

[18] M. Fowles, Black carbon sequestration as an alternative to bioenergy, *Biomass and Bioenergy*, 31 (2007) 426-432.

[19] H. Bamdad, K. Hawboldt, S. Macquarrie, A review on common adsorbents for acid gases removal: Focus on biochar, *Renewable & Sustainable Energy Reviews*, 81 (2017) S1364032117309152.

[20] M. Kumar, X. Xiong, Y. Sun, I.K.M. Yu, D.C.W. Tsang, D. Hou, J. Gupta, T. Bhaskar, A. Pandey, Critical Review on Biochar-Supported Catalysts for Pollutant Degradation and Sustainable Biorefinery, *Advanced Sustainable Systems*, (2020) 1900149.

[21] J. Lee, K.-H. Kim, E.E. Kwon, Biochar as a Catalyst, *Renewable & Sustainable Energy Reviews*, 77 (2017b) 70-79.

[22] Z. Wan, D.-W. Cho, D.C.W. Tsang, M. Li, T. Sun, F. Verpoort, Concurrent adsorption and micro-electrolysis of Cr(VI) by nanoscale zerovalent iron/biochar/Ca-alginate composite, *Environmental Pollution*, 247 (2019a) 410-420.

[23] Z. Wan, Y. Sun, D.C.W. Tsang, I.K.M. Yu, J. Fan, J.H. Clark, Y. Zhou, X. Cao, B. Gao, Y.S. Ok, A sustainable biochar catalyst synergized with copper heteroatoms and CO₂ for singlet oxygenation and electron transfer routes, *Green Chemistry*, 21 (2019b) 4800-4814.

[24] X. Li, L. Liu, X. Wang, Y.S. Ok, J.A.W. Elliott, S.X. Chang, H.-J. Chung, Flexible and Self-Healing Aqueous Supercapacitors for Low Temperature Applications: Polyampholyte Gel

936 Electrolytes with Biochar Electrodes, *Scientific reports*, 7 (2017) 1685.

937 [25] M. Ahmad, A.U. Rajapaksha, J.E. Lim, M. Zhang, N. Bolan, D. Mohan, M. Vithanage, S.S.

938 Lee, Y.S. Ok, Biochar as a sorbent for contaminant management in soil and water: A review,

939 *Chemosphere*, 99 (2014) 19-33.

940 [26] F. Beckers, Y.M. Awad, J. Beiyan, J. Abridata, S. Mothes, D.C.W. Tsang, Y.S. Ok, J.

941 Rinklebe, Impact of biochar on mobilization, methylation, and ethylation of mercury under

942 dynamic redox conditions in a contaminated floodplain soil, *Environment International*, 127 (2019)

943 276-290.

944 [27] A. El-Naggar, S.S. Lee, J. Rinklebe, M. Farooq, H. Song, A.K. Sarmah, A.R. Zimmerman,

945 M. Ahmad, S.M. Shaheen, Y.S. Ok, Biochar application to low fertility soils: A review of current

946 status, and future prospects, *Geoderma*, 337 (2019) 536-554.

947 [28] X. Chen, W.-D. Oh, T.-T. Lim, Graphene- and CNTs-based carbocatalysts in persulfates

948 activation: Material design and catalytic mechanisms, *Chemical Engineering Journal*, 354 (2018a)

949 941-976.

950 [29] H. Sun, S. Liu, G. Zhou, H.M. Ang, M.O. Tadé, S. Wang, Reduced Graphene Oxide for

951 Catalytic Oxidation of Aqueous Organic Pollutants, *ACS applied materials & interfaces*, 4 (2012)

952 5466-5471.

953 [30] H. Lee, H.I. Kim, S. Weon, W. Choi, Y.S. Hwang, J. Seo, C. Lee, J.H. Kim, Activation of

954 Persulfates by Graphitized Nanodiamonds for Removal of Organic Compounds, *Environmental*

955 *science & technology*, 50 (2016) 10134.

956 [31] X. Duan, H. Sun, S. Wang, Metal-Free Carbocatalysis in Advanced Oxidation Reactions,

957 *Accounts of Chemical Research*, 51 (2018) 678.

958 [32] A.L. Cazetta, A.M.M. Vargas, E.M. Nogami, M.H. Kunita, M.R. Guilherme, A.C. Martins,

959 T.L. Silva, J.C.G. Moraes, V.C. Almeida, NaOH-activated carbon of high surface area produced
 960 from coconut shell: Kinetics and equilibrium studies from the methylene blue adsorption,
 961 Chemical Engineering Journal, 174 (2011) 117-125.

962 [33] A.U. Rajapaksha, S.S. Chen, D.C.W. Tsang, M. Zhang, M. Vithanage, S. Mandal, B. Gao,
 963 N.S. Bolan, Y.S. Ok, Engineered/designer biochar for contaminant removal/immobilization from
 964 soil and water: Potential and implication of biochar modification, Chemosphere, 148 (2016) 276-
 965 291.

966 [34] F. Yang, S. Zhang, Y. Sun, K. Cheng, J. Li, D.C.W. Tsang, Fabrication and characterization
 967 of hydrophilic corn stalk biochar-supported nanoscale zero-valent iron composites for efficient
 968 metal removal, Bioresource technology, 265 (2018) 490-497.

969 [35] F. Yang, S. Zhang, Y. Sun, D.C.W. Tsang, K. Cheng, Y.S. Ok, Assembling biochar with
 970 various layered double hydroxides for enhancement of phosphorus recovery, Journal of hazardous
 971 materials, 365 (2019c) 665-673.

972 [36] Y. Yi, Z. Huang, B. Lu, J. Xian, E.P. Tsang, W. Cheng, J. Fang, Z. Fang, Magnetic biochar
 973 for environmental remediation: A review, Bioresource technology, 298 (2020) 122468.

974 [37] H. Wang, B. Gao, S. Wang, J. Fang, Y. Xue, K. Yang, Removal of Pb(II), Cu(II), and Cd(II)
 975 from aqueous solutions by biochar derived from KMnO₄ treated hickory wood, Bioresource
 976 technology, 197 (2015a) 356-362.

977 [38] M.-T. Yang, W.-C. Tong, J. Lee, E. Kwon, K.-Y.A. Lin, CO₂ as a reaction medium for
 978 pyrolysis of lignin leading to magnetic cobalt-embedded biochar as an enhanced catalyst for Oxone
 979 activation, Journal of colloid and interface science, 545 (2019d) 16-24.

980 [39] W.-D. Oh, T.-T. Lim, Design and application of heterogeneous catalysts as peroxydisulfate
 981 activator for organics removal: An overview, Chemical Engineering Journal, 358 (2019) 110-133.

982 [40] J. Ortiz-Medina, Z. Wang, R. Cruz-Silva, A. Morelos-Gomez, F. Wang, X. Yao, M.
983 Terrones, M. Endo, Defect Engineering and Surface Functionalization of Nanocarbons for Metal-
984 Free Catalysis, *Advanced materials*, 31 (2019) 1805717.

985 [41] B. Frank, J. Zhang, R. Blume, R. Schlögl, D.S. Su, Heteroatoms Increase the Selectivity in
986 Oxidative Dehydrogenation Reactions on Nanocarbons, *Angewandte Chemie International*
987 *Edition*, 48 (2009) 6913-6917.

988 [42] Q. Yang, Z. Xiao, D. Kong, T. Zhang, X. Duan, S. Zhou, Y. Niu, Y. Shen, H. Sun, S. Wang,
989 L. Zhi, New insight to the role of edges and heteroatoms in nanocarbons for oxygen reduction
990 reaction, *Nano Energy*, 66 (2019e) 104096.

991 [43] S. Zhu, X. Huang, F. Ma, L. Wang, X. Duan, S. Wang, Catalytic Removal of Aqueous
992 Contaminants on N-Doped Graphitic Biochars: Inherent Roles of Adsorption and Nonradical
993 Mechanisms, *Environmental science & technology*, 52 (2018) 8649-8658.

994 [44] D. Ding, S. Yang, X. Qian, L. Chen, T. Cai, Nitrogen-doping positively whilst sulfur-
995 doping negatively affect the catalytic activity of biochar for the degradation of organic contaminant,
996 *Applied Catalysis B: Environmental*, 263 (2020) 118348.

997 [45] S.-H. Ho, Y.-d. Chen, R. Li, C. Zhang, Y. Ge, G. Cao, M. Ma, X. Duan, S. Wang, N.-q.
998 Ren, N-doped graphitic biochars from C-phycocyanin extracted *Spirulina* residue for catalytic
999 persulfate activation toward nonradical disinfection and organic oxidation, *Water research*, 159
1000 (2019) 77-86.

1001 [46] D. Li, Y. Jia, G. Chang, J. Chen, H. Liu, J. Wang, Y. Hu, Y. Xia, D. Yang, X. Yao, A
1002 Defect-Driven Metal-free Electrocatalyst for Oxygen Reduction in Acidic Electrolyte, *Chem*, 4
1003 (2018) 2345-2356.

1004 [47] X. Liu, L. Dai, Carbon-based metal-free catalysts, *Nature Reviews Materials*, 1 (2016)

1005 16064.

1006 [48] T.S. Miller, A.B. Jorge, T.M. Suter, A. Sella, F. Corà, P.F. McMillan, Carbon nitrides:
 1007 synthesis and characterization of a new class of functional materials, *Physical Chemistry Chemical*
 1008 *Physics*, 19 (2017) 15613-15638.

1009 [49] M.M. Mian, G. Liu, B. Yousaf, B. Fu, R. Ahmed, Q. Abbas, M.A.M. Munir, L. Ruijia,
 1010 One-step synthesis of N-doped metal/biochar composite using NH₃-ambiance pyrolysis for
 1011 efficient degradation and mineralization of Methylene Blue, *Journal of Environmental Sciences*,
 1012 78 (2019) 29-41.

1013 [50] M.M. Mian, G. Liu, B. Yousaf, B. Fu, H. Ullah, M.U. Ali, Q. Abbas, M.A. Mujtaba Munir,
 1014 L. Ruijia, Simultaneous functionalization and magnetization of biochar via NH₃ ambiance
 1015 pyrolysis for efficient removal of Cr (VI), *Chemosphere*, 208 (2018) 712-721.

1016 [51] X. Duan, H. Sun, Y. Wang, K. Jian, S. Wang, N-Doping-Induced Nonradical Reaction on
 1017 Single-Walled Carbon Nanotubes for Catalytic Phenol Oxidation, *Acs Catalysis*, 5 (2015a) 553-
 1018 559.

1019 [52] K. Gao, B. Wang, L. Tao, B.V. Cuning, Z. Zhang, S. Wang, R.S. Ruoff, L. Qu, Efficient
 1020 Metal-Free Electrocatalysts from N-Doped Carbon Nanomaterials: Mono-Doping and Co-Doping,
 1021 *Advanced materials*, 31 (2019) 1805121.

1022 [53] X. Duan, Z. Ao, H. Sun, L. Zhou, G. Wang, S. Wang, Insights into N-doping in single-
 1023 walled carbon nanotubes for enhanced activation of superoxides: a mechanistic study, *Chemical*
 1024 *Communications*, 51 (2015b) 15249-15252.

1025 [54] H. Sun, C.K. Kwan, A. Suvorova, H.M. Ang, M.O. Tadé, S. Wang, Catalytic oxidation of
 1026 organic pollutants on pristine and surface nitrogen-modified carbon nanotubes with sulfate radicals,
 1027 *Applied Catalysis B Environmental*, 154-155 (2014) 134-141.

1028 [55] Z. Wan, Y. Sun, D.C.W. Tsang, D. Hou, X. Cao, S. Zhang, B. Gao, Y.S. Ok, Sustainable
 1029 remediation with electroactive biochar system: Mechanisms and perspectives, *Green Chemistry*,
 1030 (2020a)

1031 [56] D. Wu, W. Song, L. Chen, X. Duan, Q. Xia, X. Fan, Y. Li, F. Zhang, W. Peng, S. Wang,
 1032 High-performance porous graphene from synergetic nitrogen doping and physical activation for
 1033 advanced nonradical oxidation, *Journal of hazardous materials*, 381 (2020) 121010.

1034 [57] J. Liang, D. Tang, L. Huang, Y. Chen, W. Ren, J. Sun, High oxygen reduction reaction
 1035 performance nitrogen-doped biochar cathode: A strategy for comprehensive utilizing nitrogen and
 1036 carbon in water hyacinth, *Bioresource technology*, 267 (2018) 524-531.

1037 [58] M. Shao, Q. Chang, J.-P. Dodelet, R. Chenitz, Recent Advances in Electrocatalysts for
 1038 Oxygen Reduction Reaction, *Chemical Reviews*, 116 (2016) 3594-3657.

1039 [59] L.-L. Ling, W.-J. Liu, S. Zhang, H. Jiang, Magnesium Oxide Embedded Nitrogen Self-
 1040 Doped Biochar Composites: Fast and High-Efficiency Adsorption of Heavy Metals in an Aqueous
 1041 Solution, *Environmental science & technology*, 51 (2017) 10081-10089.

1042 [60] X. Rong, M. Xie, L. Kong, V. Natarajan, L. Ma, J. Zhan, The magnetic biochar derived
 1043 from banana peels as a persulfate activator for organic contaminants degradation, *Chemical*
 1044 *Engineering Journal*, 372 (2019) 294-303.

1045 [61] W. Ma, N. Wang, Y. Du, P. Xu, B. Sun, L. Zhang, K.-Y.A. Lin, Human-Hair-Derived N,
 1046 S-Doped Porous Carbon: An Enrichment and Degradation System for Wastewater Remediation in
 1047 the Presence of Peroxymonosulfate, *ACS Sustainable Chemistry & Engineering*, 7 (2019) 2718-
 1048 2727.

1049 [62] Y. Xie, W. Hu, X. Wang, W. Tong, P. Li, H. Zhou, Y. Wang, Y. Zhang, Molten salt induced
 1050 nitrogen-doped biochar nanosheets as highly efficient peroxymonosulfate catalyst for organic

1051 pollutant degradation, *Environmental Pollution*, 260 (2020) 114053.

1052 [63] J. Liu, S. Jiang, D. Chen, L. Liu, J. Wu, Y. Shu, Activation of persulfate with biochar for
 1053 degradation of bisphenol A in soil, *Chemical Engineering Journal*, (2019a) 122637.

1054 [64] J. Yu, L. Tang, Y. Pang, G. Zeng, J. Wang, Y. Deng, Y. Liu, H. Feng, S. Chen, X. Ren,
 1055 Magnetic nitrogen-doped sludge-derived biochar catalysts for persulfate activation: Internal
 1056 electron transfer mechanism, *Chemical Engineering Journal*, 364 (2019a) 146-159.

1057 [65] K. Luo, Q. Yang, Y. Pang, D. Wang, X. Li, M. Lei, Q. Huang, Unveiling the mechanism
 1058 of biochar-activated hydrogen peroxide on the degradation of ciprofloxacin, *Chemical Engineering*
 1059 *Journal*, 374 (2019) 520-530.

1060 [66] W.-D. Oh, G. Lisak, R.D. Webster, Y.-N. Liang, A. Veksha, A. Giannis, J.G.S. Moo, J.-W.
 1061 Lim, T.-T. Lim, Insights into the thermolytic transformation of lignocellulosic biomass waste to
 1062 redox-active carbocatalyst: Durability of surface active sites, *Applied Catalysis B: Environmental*,
 1063 233 (2018) 120-129.

1064 [67] Z. Lin, G. Waller, L. Yan, M. Liu, C.i. Wong, Facile Synthesis of Nitrogen-Doped
 1065 Graphene via Pyrolysis of Graphene Oxide and Urea, and its Electrocatalytic Activity toward the
 1066 Oxygen-Reduction Reaction, *Advanced Energy Materials*, 2 (2012) 884-888.

1067 [68] H. Wang, W. Guo, B. Liu, Q. Wu, H. Luo, Q. Zhao, Q. Si, F. Sseguya, N. Ren, Edge-
 1068 nitrogenated biochar for efficient peroxydisulfate activation: An electron transfer mechanism,
 1069 *Water research*, 160 (2019a) 405-414.

1070 [69] J. Hou, T. Jiang, R. Wei, F. Idrees, D. Bahnemann, Ultrathin-Layer Structure of BiOI
 1071 Microspheres Decorated on N-Doped Biochar With Efficient Photocatalytic Activity, *Frontiers in*
 1072 *Chemistry*, 7 (2019)

1073 [70] W. Chen, H. Yang, Y. Chen, X. Chen, Y. Fang, H. Chen, Biomass pyrolysis for nitrogen-

1074 containing liquid chemicals and nitrogen-doped carbon materials, *Journal of Analytical and*
1075 *Applied Pyrolysis*, 120 (2016) 186-193.

1076 [71] Z. Jin, B. Wang, L. Ma, P. Fu, L. Xie, X. Jiang, W. Jiang, Air pre-oxidation induced high
1077 yield N-doped porous biochar for improving toluene adsorption, *Chemical Engineering Journal*,
1078 385 (2020) 123843.

1079 [72] W. Yu, F. Lian, G. Cui, Z. Liu, N-doping effectively enhances the adsorption capacity of
1080 biochar for heavy metal ions from aqueous solution, *Chemosphere*, 193 (2018) 8-16.

1081 [73] F. Lian, G. Cui, Z. Liu, L. Duo, G. Zhang, B. Xing, One-step synthesis of a novel N-doped
1082 microporous biochar derived from crop straws with high dye adsorption capacity, *Journal of*
1083 *environmental management*, 176 (2016) 61-68.

1084 [74] Q. Zhou, X. Jiang, X. Li, C.Q. Jia, W. Jiang, Preparation of high-yield N-doped biochar
1085 from nitrogen-containing phosphate and its effective adsorption for toluene, *RSC advances*, 8
1086 (2018) 30171-30179.

1087 [75] X. Wang, Y. Liu, L. Zhu, Y. Li, K. Wang, K. Qiu, N. Tippayawong, P. Aggarangsi, P.
1088 Reubroycharoen, S. Wang, Biomass derived N-doped biochar as efficient catalyst supports for
1089 CO₂ methanation, *Journal of CO₂ Utilization*, 34 (2019b) 733-741.

1090 [76] X. Chen, X. Duan, W.-D. Oh, P.-H. Zhang, C.-T. Guan, Y.-A. Zhu, T.-T. Lim, Insights into
1091 nitrogen and boron-co-doped graphene toward high-performance peroxymonosulfate activation:
1092 Maneuverable N-B bonding configurations and oxidation pathways, *Applied Catalysis B:*
1093 *Environmental*, 253 (2019) 419-432.

1094 [77] J.R.J. Zaeni, J.-W. Lim, Z. Wang, D. Ding, Y.-S. Chua, S.-L. Ng, W.-D. Oh, In situ nitrogen
1095 functionalization of biochar via one-pot synthesis for catalytic peroxymonosulfate activation:
1096 Characteristics and performance studies, *Separation and Purification Technology*, 241 (2020)

1097 116702.

1098 [78] Y. Wang, L. Chen, C. Chen, J. Xi, H. Cao, X. Duan, Y. Xie, W. Song, S. Wang, Occurrence
 1099 of both hydroxyl radical and surface oxidation pathways in N-doped layered nanocarbons for
 1100 aqueous catalytic ozonation, *Applied Catalysis B: Environmental*, 254 (2019c) 283-291.

1101 [79] X. Duan, S. Indrawirawan, H. Sun, S. Wang, Effects of nitrogen-, boron-, and phosphorus-
 1102 doping or codoping on metal-free graphene catalysis, *Catalysis Today*, 249 (2015c) 184-191.

1103 [80] X. Duan, K. O'Donnell, H. Sun, Y. Wang, S. Wang, Sulfur and Nitrogen Co-Doped
 1104 Graphene for Metal-Free Catalytic Oxidation Reactions, *Small*, 11 (2015d) 3036-3044.

1105 [81] J. Liang, Y. Jiao, M. Jaroniec, S.Z. Qiao, Sulfur and Nitrogen Dual-Doped Mesoporous
 1106 Graphene Electrocatalyst for Oxygen Reduction with Synergistically Enhanced Performance,
 1107 *Angewandte Chemie International Edition*, 51 (2012) 11496-11500.

1108 [82] Y. Zhao, L. Yang, S. Chen, X. Wang, Y. Ma, Q. Wu, Y. Jiang, W. Qian, Z. Hu, Can Boron
 1109 and Nitrogen Co-doping Improve Oxygen Reduction Reaction Activity of Carbon Nanotubes?,
 1110 *Journal of the American Chemical Society*, 135 (2013) 1201-1204.

1111 [83] X.-k. Ma, N.-H. Lee, H.-J. Oh, S.-C. Jung, W.-J. Lee, S.-J. Kim, Morphology control of
 1112 hexagonal boron nitride by a silane coupling agent, *Journal of Crystal Growth*, 316 (2011) 185-
 1113 190.

1114 [84] Q. Zhong, Q. Lin, R. Huang, H. Fu, X. Zhang, H. Luo, R. Xiao, Oxidative degradation of
 1115 tetracycline using persulfate activated by N and Cu codoped biochar, *Chemical Engineering*
 1116 *Journal*, 380 (2020) 122608.

1117 [85] M. Sevilla, A.B. Fuertes, The production of carbon materials by hydrothermal
 1118 carbonization of cellulose, *Carbon*, 47 (2009) 2281-2289.

1119 [86] L. Wang, W. Yan, C. He, H. Wen, Z. Cai, Z. Wang, Z. Chen, W. Liu, Microwave-assisted

1120 preparation of nitrogen-doped biochars by ammonium acetate activation for adsorption of acid red
 1121 18, *Applied Surface Science*, 433 (2018a) 222-231.

1122 [87] Z. Wan, Y. Sun, D.C.W. Tsang, Z. Xu, E. Khan, S.-H. Liu, X. Cao, Sustainable impact of
 1123 tartaric acid as electron shuttle on hierarchical iron-incorporated biochar, *Chemical Engineering*
 1124 *Journal*, 395 (2020b) 125138.

1125 [88] X. Xu, Y. Zheng, B. Gao, X. Cao, N-doped biochar synthesized by a facile ball-milling
 1126 method for enhanced sorption of CO₂ and reactive red, *Chemical Engineering Journal*, 368 (2019b)
 1127 564-572.

1128 [89] Y. Gao, S. Xu, Q. Yue, S. Ortoboy, B. Gao, Y. Sun, Synthesis and characterization of
 1129 heteroatom-enriched biochar from keratin-based and algous-based wastes, *Advanced Powder*
 1130 *Technology*, 27 (2016) 1280-1286.

1131 [90] L. Xu, C. Wu, P. Liu, X. Bai, X. Du, P. Jin, L. Yang, X. Jin, X. Shi, Y. Wang,
 1132 Peroxymonosulfate activation by nitrogen-doped biochar from sawdust for the efficient
 1133 degradation of organic pollutants, *Chemical Engineering Journal*, 387 (2020) 124065.

1134 [91] Y. Sun, I.K.M. Yu, D.C.W. Tsang, X. Cao, D. Lin, L. Wang, N.J.D. Graham, D.S. Alessi,
 1135 M. Komárek, Y.S. Ok, Y. Feng, X.-D. Li, Multifunctional iron-biochar composites for the removal
 1136 of potentially toxic elements, inherent cations, and hetero-chloride from hydraulic fracturing
 1137 wastewater, *Environment International*, 124 (2019) 521-532.

1138 [92] Y. Sun, S.S. Chen, A.Y.T. Lau, D.C.W. Tsang, S.K. Mohanty, A. Bhatnagar, J. Rinklebe,
 1139 K.-Y.A. Lin, Y.S. Ok, Waste-derived compost and biochar amendments for stormwater treatment
 1140 in bioretention column: Co-transport of metals and colloids, *Journal of hazardous materials*, 383
 1141 (2020) 121243.

1142 [93] D. Zhong, Y. Jiang, Z. Zhao, L. Wang, J. Chen, S. Ren, Z. Liu, Y. Zhang, D.C.W. Tsang,

1143 J.C. Crittenden, pH Dependence of Arsenic Oxidation by Rice-Husk-Derived Biochar: Roles of
 1144 Redox-Active Moieties, *Environmental science & technology*, 53 (2019a) 9034-9044.

1145 [94] S. Guo, Y. Gao, Y. Wang, Z. Liu, X. Wei, P. Peng, B. Xiao, Y. Yang, Urea/ZnCl₂ in situ
 1146 hydrothermal carbonization of *Camellia sinensis* waste to prepare N-doped biochar for heavy
 1147 metal removal, *Environmental Science and Pollution Research*, 26 (2019) 30365-30373.

1148 [95] C. Gai, Y. Guo, N. Peng, T. Liu, Z. Liu, N-Doped biochar derived from co-hydrothermal
 1149 carbonization of rice husk and *Chlorella pyrenoidosa* for enhancing copper ion adsorption, *RSC*
 1150 *Advances*, 6 (2016) 53713-53722.

1151 [96] F. Yang, L. Sun, W. Xie, Q. Jiang, Y. Gao, W. Zhang, Y. Zhang, Nitrogen-functionalization
 1152 biochars derived from wheat straws via molten salt synthesis: An efficient adsorbent for atrazine
 1153 removal, *Science of The Total Environment*, 607-608 (2017) 1391-1399.

1154 [97] Y. Li, B. Xing, X. Wang, K. Wang, L. Zhu, S. Wang, Nitrogen-Doped Hierarchical Porous
 1155 Biochar Derived from Corn Stalks for Phenol-Enhanced Adsorption, *Energy & Fuels*, 33 (2019a)
 1156 12459-12468.

1157 [98] J. Lu, C. Zhang, J. Wu, Y. Luo, Adsorptive Removal of Bisphenol A Using N-Doped
 1158 Biochar Made of *Ulva prolifera*, *Water, Air, & Soil Pollution*, 228 (2017) 327.

1159 [99] M.V. Nguyen, B.K. Lee, A Novel removal of CO₂ using nitrogen doped biochar beads as
 1160 a green adsorbent, *Process Safety & Environmental Protection*, 104 (2016) 490-498.

1161 [100] D. Wang, Y. Sun, D.C.W. Tsang, E. Khan, D.-W. Cho, Y. Zhou, F. Qi, J. Gong, L. Wang,
 1162 Synergistic utilization of inherent halides and alcohols in hydraulic fracturing wastewater for
 1163 radical-based treatment: A case study of di-(2-ethylhexyl) phthalate removal, *Journal of hazardous*
 1164 *materials*, 384 (2020) 121321.

1165 [101] X. Duan, Z. Ao, H. Sun, S. Indrawirawan, Y. Wang, J. Kang, F. Liang, J. Zhu, S. Wang,

1166 Nitrogen-Doped Graphene for Generation and Evolution of Reactive Radicals by Metal-Free
 1167 Catalysis, ACS applied materials & interfaces, 7 (2015e) 4169.

1168 [102] Z. Li, Y. Sun, Y. Yang, Y. Han, T. Wang, J. Chen, D.C.W. Tsang, Biochar-supported
 1169 nanoscale zero-valent iron as an efficient catalyst for organic degradation in groundwater, Journal
 1170 of hazardous materials, 383 (2020) 121240.

1171 [103] B. Pan, H. Li, D. Lang, B. Xing, Environmentally persistent free radicals: Occurrence,
 1172 formation mechanisms and implications, Environmental Pollution, 248 (2019) 320-331.

1173 [104] X. Ruan, Y. Sun, W. Du, Y. Tang, Q. Liu, Z. Zhang, W. Doherty, R.L. Frost, G. Qian,
 1174 D.C.W. Tsang, Formation, characteristics, and applications of environmentally persistent free
 1175 radicals in biochars: A review, Bioresource technology, 281 (2019) 457-468.

1176 [105] X. Duan, Z. Ao, L. Zhou, H. Sun, G. Wang, S. Wang, Occurrence of radical and nonradical
 1177 pathways from carbocatalysts for aqueous and nonaqueous catalytic oxidation, Applied Catalysis
 1178 B: Environmental, 188 (2016) 98-105.

1179 [106] X. Duan, H. Sun, K. Jian, Y. Wang, S. Wang, Insights into Heterogeneous Catalysis of
 1180 Persulfate Activation on Dimensional-Structured Nanocarbons, Acs Catalysis, 5 (2015f) 4629-
 1181 4636.

1182 [107] C. Liu, L. Chen, D. Ding, T. Cai, From rice straw to magnetically recoverable nitrogen
 1183 doped biochar: Efficient activation of peroxymonosulfate for the degradation of metolachlor,
 1184 Applied Catalysis B: Environmental, 254 (2019b) 312-320.

1185 [108] F. Yao, Q. Yang, M. Yan, X. Li, F. Chen, Y. Zhong, H. Yin, S. Chen, J. Fu, D. Wang, X.
 1186 Li, Synergistic adsorption and electrocatalytic reduction of bromate by Pd/N-doped loofah sponge-
 1187 derived biochar electrode, Journal of hazardous materials, 386 (2020) 121651.

1188 [109] Y.-X. Liu, S.-M. Du, J. Cao, W.-s. Huang, X.-R. Zhang, B.-P. Qi, S.-H. Zhang,

1189 Simultaneous Determination of Hydroquinone and Catechol by N-doped Porous Biochar-modified
 1190 Electrode, *Bulletin of the Korean Chemical Society*, 41 (2020) 261-265.

1191 [110] M. Wang, Y. Lai, J. Fang, J. Li, F. Qin, K. Zhang, H. Lu, N-doped porous carbon derived
 1192 from biomass as an advanced electrocatalyst for aqueous aluminium/air battery, *International*
 1193 *Journal of Hydrogen Energy*, 40 (2015b) 16230-16237.

1194 [111] Y. Li, L. Liu, R. Shi, S. Yang, C. Zhao, Y. Shi, C. Cao, X. Yan, Natural Okra Shells
 1195 Derived Nitrogen-Doped Porous Carbon to Regulate Polysulfides for High-Performance Lithium–
 1196 Sulfur Batteries, *Energy Technology*, 7 (2019b) 1900165.

1197 [112] M. Borghei, N. Laocharoen, E. Kibena-Pöldsepp, L.-S. Johansson, J. Campbell, E.
 1198 Kauppinen, K. Tammeveski, O.J. Rojas, Porous N,P-doped carbon from coconut shells with high
 1199 electrocatalytic activity for oxygen reduction: Alternative to Pt-C for alkaline fuel cells, *Applied*
 1200 *Catalysis B: Environmental*, 204 (2017) 394-402.

1201 [113] K. An, X. Xu, X. Liu, Mo₂C-Based Electrocatalyst with Biomass-Derived Sulfur and
 1202 Nitrogen Co-Doped Carbon as a Matrix for Hydrogen Evolution and Organic Pollutant Removal,
 1203 *ACS Sustainable Chemistry & Engineering*, 6 (2018) 1446-1455.

1204 [114] Y. Zhou, Y. Leng, W. Zhou, J. Huang, M. Zhao, J. Zhan, C. Feng, Z. Tang, S. Chen, H.
 1205 Liu, Sulfur and nitrogen self-doped carbon nanosheets derived from peanut root nodules as high-
 1206 efficiency non-metal electrocatalyst for hydrogen evolution reaction, *Nano Energy*, 16 (2015) 357-
 1207 366.

1208 [115] X. Liu, Y. Zhou, W. Zhou, L. Li, S. Huang, S. Chen, Biomass-derived nitrogen self-doped
 1209 porous carbon as effective metal-free catalysts for oxygen reduction reaction, *Nanoscale*, 7 (2015a)
 1210 6136-6142.

1211 [116] P. Chen, L.-K. Wang, G. Wang, M.-R. Gao, J. Ge, W.-J. Yuan, Y.-H. Shen, A.-J. Xie, S.-

1212 H. Yu, Nitrogen-doped nanoporous carbon nanosheets derived from plant biomass: an efficient
 1213 catalyst for oxygen reduction reaction, *Energy & Environmental Science*, 7 (2014) 4095-4103.

1214 [117] F. Liu, H. Peng, C. You, Z. Fu, P. Huang, H. Song, S. Liao, High-Performance Doped
 1215 Carbon Catalyst Derived from Nori Biomass with Melamine Promoter, *Electrochimica Acta*, 138
 1216 (2014) 353-359.

1217 [118] F. Pan, Z. Cao, Q. Zhao, H. Liang, J. Zhang, Nitrogen-doped porous carbon nanosheets
 1218 made from biomass as highly active electrocatalyst for oxygen reduction reaction, *Journal of*
 1219 *Power Sources*, 272 (2014) 8-15.

1220 [119] L. Pi, R. Jiang, W. Cai, L. Wang, Y. Wang, J. Cai, X. Mao, Bionic Preparation of CeO₂-
 1221 Encapsulated Nitrogen Self-Doped Biochars for Highly Efficient Oxygen Reduction, *ACS applied*
 1222 *materials & interfaces*, 12 (2020) 3642-3653.

1223 [120] M. Zhang, X. Jin, L. Wang, M. Sun, Y. Tang, Y. Chen, Y. Sun, X. Yang, P. Wan,
 1224 Improving biomass-derived carbon by activation with nitrogen and cobalt for supercapacitors and
 1225 oxygen reduction reaction, *Applied Surface Science*, 411 (2017) 251-260.

1226 [121] W.-J. Liu, H. Jiang, H.-Q. Yu, Emerging applications of biochar-based materials for
 1227 energy storage and conversion, *Energy & Environmental Science*, 12 (2019c) 1751-1779.

1228 [122] G. Wang, Y. Deng, J. Yu, L. Zheng, L. Du, H. Song, S. Liao, From Chlorella to Nestlike
 1229 Framework Constructed with Doped Carbon Nanotubes: A Biomass-Derived, High-Performance,
 1230 Bifunctional Oxygen Reduction/Evolution Catalyst, *ACS applied materials & interfaces*, 9 (2017)
 1231 32168-32178.

1232 [123] K. Wang, S. Zhang, Z. Chen, R. Bao, Interactive effect of electrode potential on pollutants
 1233 conversion in denitrifying sulfide removal microbial fuel cells, *Chemical Engineering Journal*, 339
 1234 (2018b) 442-449.

1235 [124] T. Huggins, H. Wang, J. Kearns, P. Jenkins, Z.J. Ren, Biochar as a sustainable electrode
1236 material for electricity production in microbial fuel cells, *Bioresource technology*, 157 (2014) 114-
1237 119.

1238 [125] K. Zhong, M. Li, Y. Yang, H. Zhang, B. Zhang, J. Tang, J. Yan, M. Su, Z. Yang, Nitrogen-
1239 doped biochar derived from watermelon rind as oxygen reduction catalyst in air cathode microbial
1240 fuel cells, *Applied Energy*, 242 (2019b) 516-525.

1241 [126] T.M. Huggins, J.J. Pietron, H. Wang, Z.J. Ren, J.C. Biffinger, Graphitic biochar as a
1242 cathode electrocatalyst support for microbial fuel cells, *Bioresource technology*, 195 (2015) 147-
1243 153.

1244 [127] G. Yue, K. Meng, Q. Liu, One-Step Synthesis of N-Doped Carbon and Its Application as
1245 a Cost-Efficient Catalyst for the Oxygen Reduction Reaction in Microbial Fuel Cells,
1246 *ChemPlusChem*, 80 (2015) 1133-1138.

1247 [128] Q. Liu, Y. Zhou, S. Chen, Z. Wang, H. Hou, F. Zhao, Cellulose-derived nitrogen and
1248 phosphorus dual-doped carbon as high performance oxygen reduction catalyst in microbial fuel
1249 cell, *Journal of Power Sources*, 273 (2015b) 1189-1193.

1250 [129] L. Klüpfel, M. Keiluweit, M. Kleber, M. Sander, Redox Properties of Plant Biomass-
1251 Derived Black Carbon (Biochar), *Environmental science & technology*, 48 (2014) 5601-5611.

1252 [130] T. Sun, B.D.A. Levin, J.J.L. Guzman, A. Enders, D.A. Muller, L.T. Angenent, J. Lehmann,
1253 Rapid electron transfer by the carbon matrix in natural pyrogenic carbon, *Nature Communications*,
1254 8 (2017) 14873.

1255 [131] J.R. Miller, P. Simon, Electrochemical Capacitors for Energy Management, *Science*, 321
1256 (2008) 651.

1257 [132] M. Biswal, A. Banerjee, M. Deo, S. Ogale, From dead leaves to high energy density

1258 supercapacitors, *Energy & Environmental Science*, 6 (2013) 1249-1259.

1259 [133] Z. Li, L. Zhang, B.S. Amirkhiz, X. Tan, Z. Xu, H. Wang, B.C. Olsen, C.M.B. Holt, D.

1260 Mitlin, Carbonized Chicken Eggshell Membranes with 3D Architectures as High-Performance

1261 Electrode Materials for Supercapacitors, *Advanced Energy Materials*, 2 (2012) 431-437.

1262 [134] J. Liu, Y. Deng, X. Li, L. Wang, Promising Nitrogen-Rich Porous Carbons Derived from

1263 One-Step Calcium Chloride Activation of Biomass-Based Waste for High Performance

1264 Supercapacitors, *ACS Sustainable Chemistry & Engineering*, 4 (2016) 177-187.

1265 [135] D. Hulicova-Jurcakova, M. Seredych, G.Q. Lu, T.J. Bandosz, Combined Effect of

1266 Nitrogen- and Oxygen-Containing Functional Groups of Microporous Activated Carbon on its

1267 Electrochemical Performance in Supercapacitors, *Advanced Functional Materials*, 19 (2009) 438-

1268 447.

1269 [136] Y.-H. Lee, K.-H. Chang, C.-C. Hu, Differentiate the pseudocapacitance and double-layer

1270 capacitance contributions for nitrogen-doped reduced graphene oxide in acidic and alkaline

1271 electrolytes, *Journal of Power Sources*, 227 (2013) 300-308.

1272 [137] L. Wang, X. Li, J. Ma, Q. Wu, X. Duan, Non-activated, N, S-co-doped biochar derived

1273 from banana with superior capacitive properties, *Sustainable Energy*, 2 (2014) 39-43.

1274 [138] L. Cao, I.K.M. Yu, D.-W. Cho, D. Wang, D.C.W. Tsang, S. Zhang, S. Ding, L. Wang,

1275 Y.S. Ok, Microwave-assisted low-temperature hydrothermal treatment of red seaweed (*Gracilaria*

1276 *lemaneiformis*) for production of levulinic acid and algae hydrochar, *Bioresource technology*, 273

1277 (2019) 251-258.

1278 [139] I.K.M. Yu, D.C.W. Tsang, A.C.K. Yip, S.S. Chen, Y.S. Ok, C.S. Poon, Valorization of

1279 food waste into hydroxymethylfurfural: Dual role of metal ions in successive conversion steps,

1280 *Bioresource technology*, 219 (2016) 338-347.

1281 [140] J.B. Binder, A.V. Cefali, J.J. Blank, R.T. Raines, Mechanistic insights on the conversion
 1282 of sugars into 5-hydroxymethylfurfural, *Energy & Environmental Science*, 3 (2010) 765-771.

1283 [141] I.K.M. Yu, X. Xiong, D.C.W. Tsang, L. Wang, A.J. Hunt, H. Song, J. Shang, Y.S. Ok,
 1284 C.S. Poon, Aluminium-biochar composites as sustainable heterogeneous catalysts for glucose
 1285 isomerisation in a biorefinery, *Green Chemistry*, 21 (2019b) 1267-1281.

1286 [142] S.S. Chen, I.K.M. Yu, D.-W. Cho, H. Song, D.C.W. Tsang, J.-P. Tessonnier, Y.S. Ok,
 1287 C.S. Poon, Selective Glucose Isomerization to Fructose via a Nitrogen-doped Solid Base Catalyst
 1288 Derived from Spent Coffee Grounds, *ACS Sustainable Chemistry & Engineering*, 6 (2018b)
 1289 16113-16120.

1290 [143] J.A.H. Dreyer, P. Li, L. Zhang, G.K. Beh, R. Zhang, P.H.L. Sit, W.Y. Teoh, Influence of
 1291 the oxide support reducibility on the CO₂ methanation over Ru-based catalysts, *Applied Catalysis*
 1292 *B: Environmental*, 219 (2017) 715-726.

1293 [144] L. Roldán, Y. Marco, E. García-Bordejé, Origin of the Excellent Performance of Ru on
 1294 Nitrogen-Doped Carbon Nanofibers for CO₂ Hydrogenation to CH₄, *ChemSusChem*, 10 (2017)
 1295 1139-1144.

1296 [145] W. Zhang, Y. Li, X. Fan, F. Zhang, G. Zhang, Y.-A. Zhu, W. Peng, S. Wang, X. Duan,
 1297 Synergy of nitrogen doping and structural defects on hierarchically porous carbons toward
 1298 catalytic oxidation via a non-radical pathway, *Carbon*, 155 (2019) 268-278.

1299 [146] T.C. Nagaiah, S. Kundu, M. Bron, M. Muhler, W. Schuhmann, Nitrogen-doped carbon
 1300 nanotubes as a cathode catalyst for the oxygen reduction reaction in alkaline medium,
 1301 *Electrochemistry Communications*, 12 (2010) 338-341.

1302 [147] H.-S. Oh, J.-G. Oh, W.H. Lee, H.-J. Kim, H. Kim, The influence of the structural
 1303 properties of carbon on the oxygen reduction reaction of nitrogen modified carbon based catalysts,

1304 International Journal of Hydrogen Energy, 36 (2011) 8181-8186.

1305 [148] X. Duan, W. Li, Z. Ao, J. Kang, W. Tian, H. Zhang, S.-H. Ho, H. Sun, S. Wang, Origins
 1306 of boron catalysis in peroxymonosulfate activation and advanced oxidation, Journal of Materials
 1307 Chemistry A, 7 (2019) 23904-23913.

1308 [149] P. Hu, H. Su, Z. Chen, C. Yu, Q. Li, B. Zhou, P.J.J. Alvarez, M. Long, Selective
 1309 Degradation of Organic Pollutants Using an Efficient Metal-free Catalyst Derived from
 1310 Carbonized Polypyrrole via Peroxymonosulfate Activation, Environmental science & technology,
 1311 51 (2017) acs.est.7b03014.

1312 [150] W. Tian, H. Zhang, X. Duan, H. Sun, M.O. Tade, H.M. Ang, S. Wang, Nitrogen- and
 1313 Sulfur-Codoped Hierarchically Porous Carbon for Adsorptive and Oxidative Removal of
 1314 Pharmaceutical Contaminants, ACS applied materials & interfaces, 8 (2016) 7184-7193.

1315